https://doi.org/10.1093/plphys/kiae099 PLANT PHYSIOLOGY 2024: 195: 940–957

Plant Physiology®

Research Article

A long noncoding RNA functions in pumpkin fruit development through *S*-adenosyl-L-methionine synthetase

Jiaxing Tian,[1,2] **Fan Zhang**,[1,2] **Guoyu Zhang**,[1,2] **Xiaojie Li**,[1,2] **Changlong Wen**,[1,2,*] **Haizhen Li**[1,2,*]

1 Beijing Vegetable Research Center (BVRC), Beijing Academy of Agriculture and Forestry Sciences (BAAFS), Beijing, China
2 State Key Laboratory of Vegetable Biobreeding, Beijing Vegetable Research Center, Beijing Academy of Agriculture and Forestry Sciences, Beijing 100097, China

*Author for correspondence: wenchanglong@nercv.org (C.W.), lihaizhen@nercv.org (H.L.)
The author responsible for distribution of materials integral to the findings presented in this article in accordance with the policy described in the Instructions for Authors (https://academic.oup.com/plphys/pages/General-Instructions) is: Haizhen Li (lihaizhen@nercv.org).

Abstract

Long noncoding RNAs (lncRNAs) play important roles in various biological processes. However, the regulatory roles of lncRNAs underlying fruit development have not been extensively studied. The pumpkin (*Cucurbita* spp.) is a preferred model for understanding the molecular mechanisms regulating fruit development because of its variable shape and size and large inferior ovary. Here, we performed strand-specific transcriptome sequencing on pumpkin (*Cucurbita maxima* "Rimu") fruits at 6 developmental stages and identified 5,425 reliably expressed lncRNAs. Among the 332 lncRNAs that were differentially expressed during fruit development, the lncRNA MSTRG.44863.1 was identified as a negative regulator of pumpkin fruit development. MSTRG.44863.1 showed a relatively high expression level and an obvious period-specific expression pattern. Transient overexpression and silencing of MSTRG.44863.1 significantly increased and decreased the content of 1-aminocyclopropane carboxylic acid (a precursor of ethylene) and ethylene production, respectively. RNA pull-down and microscale thermophoresis assays further revealed that MSTRG.44863.1 can interact with *S*-adenosyl-L-methionine synthetase (SAMS), an enzyme in the ethylene synthesis pathway. Considering that ethylene negatively regulates fruit development, these results indicate that MSTRG.44863.1 plays an important role in the regulation of pumpkin fruit development, possibly through interacting with SAMS and affecting ethylene synthesis. Overall, our findings provide a rich resource for further study of fruit-related lncRNAs while offering insights into the regulation of fruit development in plants.

Introduction

The pumpkin (*Cucurbita* spp.), belonging to the family Cucurbitaceae, is a widely grown vegetable crop comprising 5 domesticated species, with *Cucurbita maxima*, *Cucurbita pepo*, and *Cucurbita moschata* being the commonly cultivated species globally. Pumpkin fruits play important roles both economically and nutritionally. Because of their long storage life and high nutritive value, pumpkins are produced for the fresh market and are valuable for food processing (Hosen et al. 2021). Thus, an understanding of the molecular mechanisms underlying the development of pumpkins will help to produce varieties with higher yield and better fruit quality. In addition, due to the large inferior ovary and variable shape and size of the fruit, the pumpkin is an ideal model species for studying fruit development. However, only a few genes related to pumpkin fruit development have been

Received October 03, 2023. Accepted January 25, 2024. Advance access publication February 28, 2024.
© The Author(s) 2024. Published by Oxford University Press on behalf of American Society of Plant Biologists.
Open Access
This is an Open Access article distributed under the terms of the Creative Commons Attribution-NonCommercial-NoDerivs licence (https://creativecommons.org/licenses/by-nc-nd/4.0/), which permits non-commercial reproduction and distribution of the work, in any medium, provided the original work is not altered or transformed in any way, and that the work is properly cited. For commercial re-use, please contact reprints@oup.com for reprints and translation rights for reprints. All other permissions can be obtained through our RightsLink service via the Permissions link on the article page on our site—for further information please contact journals.permissions@oup.com.

Downloaded from https://academic.oup.com/plphys/article/195/2/940/7615931 by Beijing Academy of Agriculture & Forestry Sciences user on 31 October 2024

identified to date, including key genes involved in sucrose biosynthesis and starch and carotenoid accumulation (Wyatt et al. 2016; Abbas et al. 2020; Wang et al. 2020b; Luo et al. 2021). More recently, several WD40 proteins were reported to be likely involved in fruit development in *C. maxima* (Chen et al. 2023a). However, given the complexity of fruit development, the role of regulatory factors in the development of pumpkins should be further revealed to elucidate the complete regulatory mechanism.

Fruits are unique plant developmental systems representing important components of human and animal diets. Horticultural characteristics such as shape, size, color, flavor, and nutrient contents influence the market value of fruits (Papoutsisa et al. 2021), which are all influenced by factors affecting fruit development. However, the underlying molecular regulation mechanism of fruit development remains to be fully elucidated. Fruit development comprises 3 phases: setting, growth, and maturation. These stages involve the regulation of numerous physiological and biochemical changes, coordinated by complex networks of genes and pathways. Recent studies on fruit development, and in particular the maturation of fleshy fruits, have led to considerable advances in their knowledge. Various genes and regulators related to fruit growth and maturation have been identified in the tomato (*Solanum lycopersicum*), a common model for the study of fleshy fruits (Giovannoni 2004; Quinet et al. 2019). For example, RIPENING INHIBITOR (RIN) was reported to play an important role in the ripening of tomato fruit (Martel et al. 2011). However, knowledge of the molecular mechanisms underlying fruit development in other fruit crops remains extremely limited.

Emerging evidence indicates that plant hormones (auxins [indole-3-acetic acid (IAA)], cytokinins, gibberellins, abscisic acid [ABA], and ethylene) can collaborate to form a complex network to regulate fruit development at different stages (Ozga and Rienecke 2003; Fenn and Giovannoni 2021). After pollination and fertilization, gibberellin, auxin, and cytokinin promote fruit setting and development by regulating cell division and expansion (Kumar et al. 2014), accompanied by a decrease in ethylene production (Shinozaki et al. 2015). Recent research offers insights into the essential role of ethylene in fruit setting and early fruit development (Martínez et al. 2013; Xin et al. 2019; Sharma et al. 2021; Boualem et al. 2022; Huang et al. 2022). Studies in Arabidopsis (*Arabidopsis thaliana*) demonstrated that early ovule abortion is associated with silique size in ethylene mutants (Carbonell-Bejerano et al. 2011). Studies in zucchini (*C. pepo*) suggest that ethylene may be a negative regulator of fruit setting and early fruit development (Martínez et al. 2013). In addition, Boualem et al. (2022) suggested that ethylene plays a dual role in cucurbits, inhibiting stamen development and elongating the ovary and fruit. Ethylene was also suggested to have a dose-dependent effect on fruit development in cucumber (*Cucumis sativus*) (Xin et al. 2019) and to exert a bidirectional regulating effect on tomato fruit size. In particular, a proper basal concentration of ethylene is optimal for fruit growth, while a lack of ethylene or excess ethylene production has an inhibitory effect on fruit growth (Huang et al. 2022). These studies indicate that ethylene plays an essential role in fruit development.

Noncoding RNAs (ncRNAs) have been revealed to be a major component of transcripts in eukaryotic genomes (Eddy 2001). Among these, long noncoding RNAs (lncRNAs) are RNA molecules with a sequence length above 200 nucleotides without apparent coding potential (Kapranov et al. 2007). In general, lncRNAs show tissue-specific and low expression, with minimal conservation among species (Wu et al. 2020). The action mechanisms of lncRNAs are complex and diverse. Recent research suggests that lncRNAs are involved in many molecular processes by interacting directly with proteins, DNA, or other RNA molecules (Lucero et al. 2021). To date, various lncRNAs have been identified and characterized in model plants such as *A. thaliana* (Liu et al. 2012; Wang et al. 2014), rice (*Oryza sativa*) (Zhang et al. 2014), and *S. lycopersicum* (Zhu et al. 2015), participating in a wide range of biological processes, such as flowering regulation (Liu et al. 2010; Chen et al. 2023b), stress responses (Zhu et al. 2014; Qin et al. 2017; Zhang et al. 2021, 2022), and fruit growth and ripening (Zhu et al. 2015; Tang et al. 2021; Yu et al. 2022). However, owing to their high diversity and low sequence conservation, knowledge of the regulatory role of plant lncRNAs remains limited.

Recent advances in next-generation sequencing technology have helped to identify several lncRNAs playing a role in fruit growth and development in various crops, including tomato (Zhu et al. 2015; Wang et al. 2018), diploid strawberry (*Fragaria vesca*) (Kang and Liu 2015), sea buckthorn (*Hippophae rhamnoides*) (Zhang et al. 2018), apple (*Malus domestica*) (Yang et al. 2019), and melon (*Cucumis melo*) (Tian et al. 2019). In tomato, a substantial delay in fruit maturation was observed following knockdown of *lncRNA1459* and *lncRNA1840* (Zhu et al. 2015; Li et al. 2018). Two lncRNAs (LNC1 and LNC2) in sea buckthorn were found to influence the biosynthesis of anthocyanin during fruit ripening (Zhang et al. 2018). A recent study showed that the lncRNA *FRILAIR* (*FRUIT RIPENING-RELATED LONG INTERGENIC RNA*) may regulate *LAC11a* (encoding a putative laccase-11-like protein) expression as a target mimic of miR397 during strawberry fruit maturation (Tang et al. 2021). Two lncRNAs, named MLNC3.2 (MSTRG.123423.2) and MLNC4.6 (MSTRG.137274.6), were found to promote the expression of the SQUAMOSA-PROMOTER BINDING PROTEIN-LIKE (SPL) transcription factors and contribute to the accumulation of anthocyanin in the skin in apple (Yang et al. 2019). Another apple lncRNA (MdLNC499), which induces the expression of *MdERF109 (ethylene response factor 109)*, plays a role in light-induced fruit coloration (Ma et al. 2021). More recently, Yu et al. (2022) proposed that MdLNC610 may be involved in regulating the production of anthocyanin induced by high light by promoting the expression of *MdACO1* (*1-aminocyclopropane-1-carboxylate oxygenase 1*) and ethylene biosynthesis. However, little is known about the

Downloaded from https://academic.oup.com/plphys/article/195/2/940/7615931 by Beijing Academy of Agriculture & Forestry Sciences user on 31 October 2024

regulation of lncRNAs associated with fruit development in cucurbit crops.

Therefore, the molecular mechanism by which lncRNAs regulate fruit development requires further investigation. Toward this end, we aimed to systematically identify and characterize the lncRNAs expressed in pumpkin fruit, with emphasis on lncRNAs associated with fruit development. Further, we conducted functional analysis of an important candidate lncRNA (MSTRG.44863.1) playing a key role in regulating the development of pumpkin fruit, possibly through interacting with *S*-adenosyl-L-methionine synthetase (SAMS) and affecting ethylene synthesis. Collectively, these findings provide a rich resource for further exploration of pumpkin lncRNAs and a perspective for studying the regulatory mechanisms of fruit development.

Results

Phenotypic data of *C. maxima* fruits

Changes in 9 fruit-related characteristics were measured during fruit development of *C. maxima* "Rimu" (Supplementary Fig. S1). The length, diameter, and pulp thickness of the fruit increased rapidly from 0 to 10 d after pollination (DAP) (Supplementary Fig. S1, A to C). The contents of fructose, glucose, and sucrose initially presented an increasing trend, and then tended to be unchanged or reduced in the later stage of fruit development (Supplementary Fig. S1, D to F). During fruit development, the starch content showed a double-peak trend at 30 DAP (2.88 ± 0.18 g/100 g fresh weight [FW]) and 50 DAP (3.34 ± 0.15 g/100 g FW; Supplementary Fig. S1G). The pumpkin fruits continuously accumulated lutein and β-carotene during development (Supplementary Fig. S1, H and I). Overall, these results indicated substantial changes in the physiology and biochemistry of pumpkins throughout their development.

Genome-wide identification and characterization of lncRNAs in *C. maxima*

Strand-specific transcriptome sequencing on *C. maxima* fruits at 6 developmental stages (Fig. 1A) was performed for systematic identification of lncRNAs based on a total of 18 libraries conducted with 3 biological replicates at each stage. Detailed information on RNA-seq data is provided in Supplementary Table S1. Approximately 88.92% to 95.52% of the reads mapped to the reference genome. A total of 5,425 candidate lncRNAs were predicted (Fig. 1B), 1,371 of which were found at all 6 developmental stages (Fig. 1C). The lncRNAs showed widespread expression on all chromosomes (Fig. 1B) with an average density of 25.65 lncRNAs per Mb. The identified lncRNAs were divided into 4 groups according to their genomic location: long inter-genic lncRNAs (lincRNAs), antisense lncRNAs, intronic lncRNAs, and sense lncRNAs (Fig. 1D). LincRNAs (69.83%) were the most abundant, while intronic lncRNAs were the least abundant (4.7%). Detailed information on the 5,425 lncRNAs is provided in Supplementary Table S2.

BLAST analysis of the 5,425 lncRNAs found in fruits of *C. maxima* against plant lncRNA databases (CANTATAdb and GreeNC) showed that the overwhelming majority (99.10%) of the identified lncRNAs were likely pumpkin-specific (Supplementary Table S3). The average guanine–cytosine (GC) content of predicted lncRNAs was 39.37%. Repeat sequence analysis indicated that most (79.67%) of the lncRNAs had no overlap with the repetitive sequences. Compared with *C. maxima* mRNAs, in general, the lncRNAs were shorter (Fig. 1E) and had lower expression levels (Fig. 1F). For example, the transcript length of the lncRNAs ranged from 202 to 13,140 nucleotides, with an average of 677 nucleotides shorter than the mRNAs of *C. maxima* (median 1,505 nucleotides).

Identification of differentially expressed lncRNAs

To identify lncRNAs involved in fruit development, we analyzed the expression levels of lncRNAs throughout fruit development at 0, 10, 20, 30, 40, and 50 DAP (Fig. 2A). Compared with 0 DAP levels, we identified 322 differentially expressed lncRNAs (DELs), including 157 lincRNAs, 81 antisense lncRNAs, 72 sense lncRNAs, and 12 intronic lncRNAs (Supplementary Table S4). Six DELs were shared across all 5 comparisons (Fig. 2A, Supplementary Fig. S2). In general, there were more downregulated DELs than upregulated DELs with the maximum number of DELs found in the 50 versus 0 DAP comparison (Fig. 2B).

The expression patterns of 8 lncRNAs were validated by reverse transcription-quantitative polymerase chain reaction (RT-qPCR). They were selected as representatives of 4 lncRNA types. Although some differences in expression levels were noted, the RT-qPCR results exhibited a trend similar to that observed in RNA-seq data (Fig. 2C). For example, both RNA-seq and RT-qPCR indicated that MSTRG.44863.1 was most highly expressed at 0 DAP. These results indicated that the identified lncRNAs were genuinely expressed.

Potential target genes and microRNAs interacting with DELs

Since lncRNAs regulate the expression of proximal or distal genes through cis- or trans-acting mechanisms, we further explored the possible interactions between DELs and target genes. Computational prediction showed 6,051 potential cis-regulated target genes for 308 DELs and 232 potential trans-regulated target genes for 143 DELs (Supplementary Table S5). Gene Ontology (GO) functional annotation of candidate target genes of the DELs identified 125 terms (Supplementary Table S6) with the top 20 terms presented in Supplementary Fig. S3, including epigenetic functions, such as histone acetylation and *S*-methyltransferase activity. The top 50 enriched Kyoto Encyclopedia of Genes and Genomes (KEGG) pathways are shown in Fig. 3A. Notably 80 potential target genes of DELs were related to the plant hormone signal transduction pathway. This suggested plant

Downloaded from https://academic.oup.com/plphys/article/195/2/940/7615931 by Beijing Academy of Agriculture & Forestry Sciences user on 31 October 2024

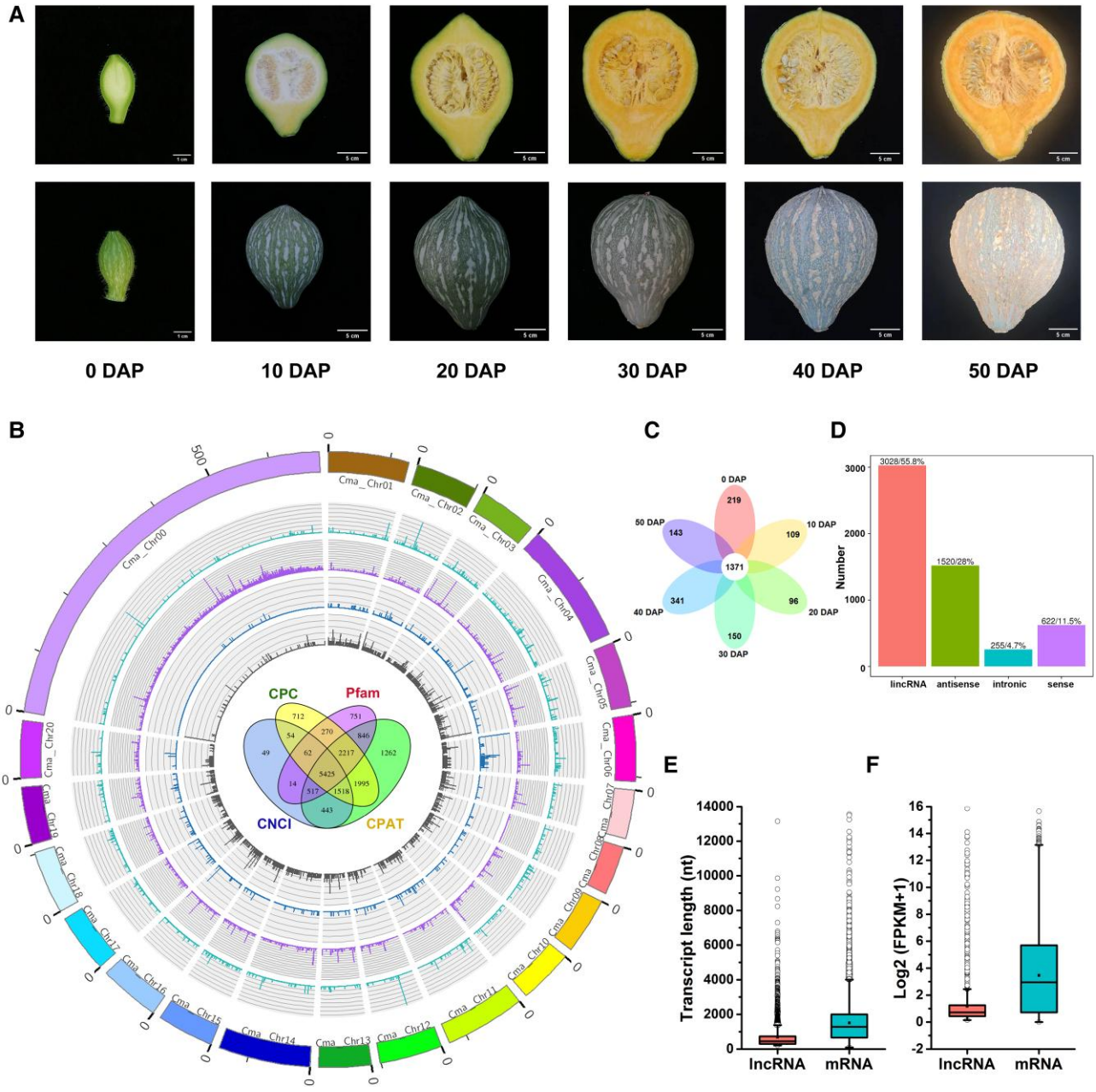

Figure 1. Characteristics of *C. maxima* lncRNAs. **A)** *C. maxima* fruits at 6 time points throughout the fruit development. **B)** Distribution of lncRNAs along *C. maxima* chromosomes. The Venn diagram in the center shows the number of lncRNAs predicted by evaluating protein-coding potential in the Coding Potential Calculator (CPC), Coding–Noncoding-Index (CNCI), Pfam scan (Pfam), and Coding Potential Assessment Tool (CPAT). In order from far to near to the Venn diagram, the first circle represents sense lncRNAs, the second circle represents lincRNAs, the third circle represents intronic lncRNAs, and the fourth circle represents antisense lncRNAs. **C)** Venn diagram of lncRNAs identified at 6 different time points. DAP represents day after pollination. **D)** Classification of *C. maxima* lncRNAs according to their genomic positions. **E and F)** Comparisons between lncRNAs and mRNAs showed that lncRNAs were shorter **E**) and had lower expression levels **F**). Central lines are medians, and box limits are the first and third quartiles. The squares in the box represent the average values. Whiskers mark the minimal (lower whisker) and maximal (upper whisker) data points within 1.5 times the interquartile range from the first and third quartiles, respectively. The points represent outliers.

hormone signal transduction is an important mechanism by which lncRNAs regulate fruit development. Therefore, co-expression analysis based on the expression levels of DELs and target genes among samples was used to construct a candidate regulatory network in the plant hormone signal transduction pathway (Fig. 3B). The proposed regulatory network consists of 242 lncRNAs interacting with potential target genes. One lncRNA might interact with 1 to 16 potential target genes suggesting a complex regulatory relationship between lncRNAs and target genes. However, further studies, especially experimental approaches, are needed to explore these potential interactions.

Downloaded from https://academic.oup.com/plphys/article/195/2/940/7615931 by Beijing Academy of Agriculture & Forestry Sciences user on 31 October 2024

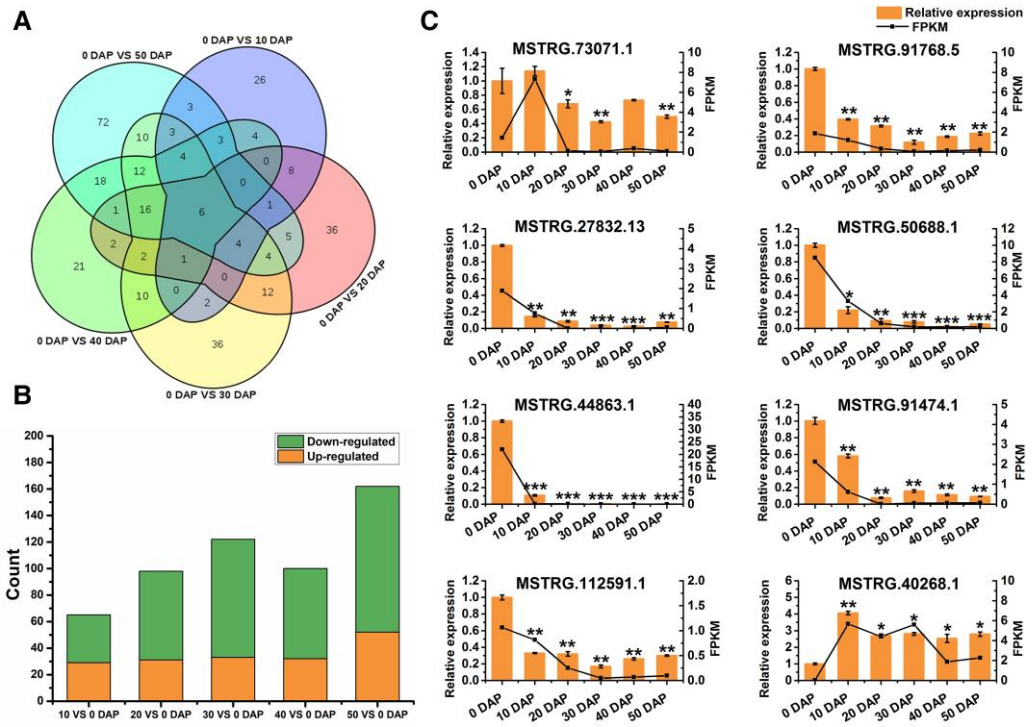

Figure 2. Identification of DELs. **A)** Venn diagram of DELs. **B)** Number of downregulated and upregulated lncRNAs. **C)** Validation of DELs. DAP, day after pollination. Error bars indicate SDs among 3 biological replicates ($n = 3$). Asterisks indicate significant differences between 2 groups (*$P < 0.05$; **$P < 0.01$; ***$P < 0.001$) calculated using paired Student's t-test. Different developmental stages were compared with 0 DAP.

Since lncRNA and microRNA (miRNA) interactions may play an important role in plants (Wu et al. 2013), all of the DELs were used to predict potential interactions with miRNAs. BLASTN identified 9 DELs as precursors to 18 known miRNAs from 6 families (Supplementary Table S7). For example, one *C. maxima* lncRNA (MSTRG.77453.2) was predicted as a precursor of cma-miR396 (Fig. 3C). In addition, psRNATarget predicted 142 lncRNAs as potential targets of 126 miRNAs belonging to 28 families (Supplementary Table S8). Among these, 6 lncRNA–miRNA pairs were identified via degradome sequencing (Supplementary Table S9). For example, MSTRG.41935.5 was a potential target of cma-miR399 and a single distinct peak was observed at the degradation site in MSTRG.41935.5 (Fig. 3, D and E). In plants, target mimicry is a regulatory mechanism that blocks the interaction of miRNAs with the original target by creating false target transcripts (target mimic) that cannot be cleaved (Wu et al. 2013). We also identified one DEL (MSTRG.41110.2) as a potential target mimic of 3 miRNAs (cma-miR160a, cma-miR160e, and cma-miR160f) belonging to the miR160 family (Fig. 3D). These results suggested that the lncRNAs might participate in the development of pumpkin fruit through interaction with miRNAs.

Full-length cloning of MSTRG.44863.1

The abovementioned results indicated that MSTRG.44863.1 has a relatively high expression level and an obvious period-specific expression pattern (Fig. 2C), indicating its potential importance in fruit development. Therefore, MSTRG.44863.1 was selected as a candidate lncRNA closely related to fruit development for further characterization.

Based on the RNA-seq data, MSTRG.44863.1 was identified as a sense lncRNA with a partial sequence. Cloning of the 3′ and 5′ ends by rapid amplification of cDNA ends (RACE), followed by full-length amplification using primers targeting both ends, showed that MSTRG.44863.1 is 1,223 nucleotides long and located on chromosome 4, containing 2 exons (Fig. 4A). The full sequence of MSTRG.44863.1 is presented in Supplementary Fig. S4. Sequence alignment showed that MSTRG.44863 partially overlaps with 2 genes in the genome (Fig. 4A). Since coding ability of RNA is an important criterion for the identification of lncRNAs, the coding potential score was calculated, indicating that MSTRG.44863.1 is a ncRNA (Supplementary Fig. S5). A search in the CANTATAdb and GreeNC databases did not identify a similar sequence in other species, indicating that MSTRG.44863.1 is a species-specific lncRNA. Moreover, sequence alignment and a BLAST search against several Cucurbitaceae species showed that the genomic sequence of MSTRG.44863 is conserved in *Cucurbita*, but is poorly conserved among other species of Cucurbitaceae.

Localization and expression analysis of MSTRG.44863.1

As the regulation mode of lncRNAs is related to their subcellular location, we further examined the subcellular location of

Downloaded from https://academic.oup.com/plphys/article/195/2/940/7615931 by Beijing Academy of Agriculture & Forestry Sciences user on 31 October 2024

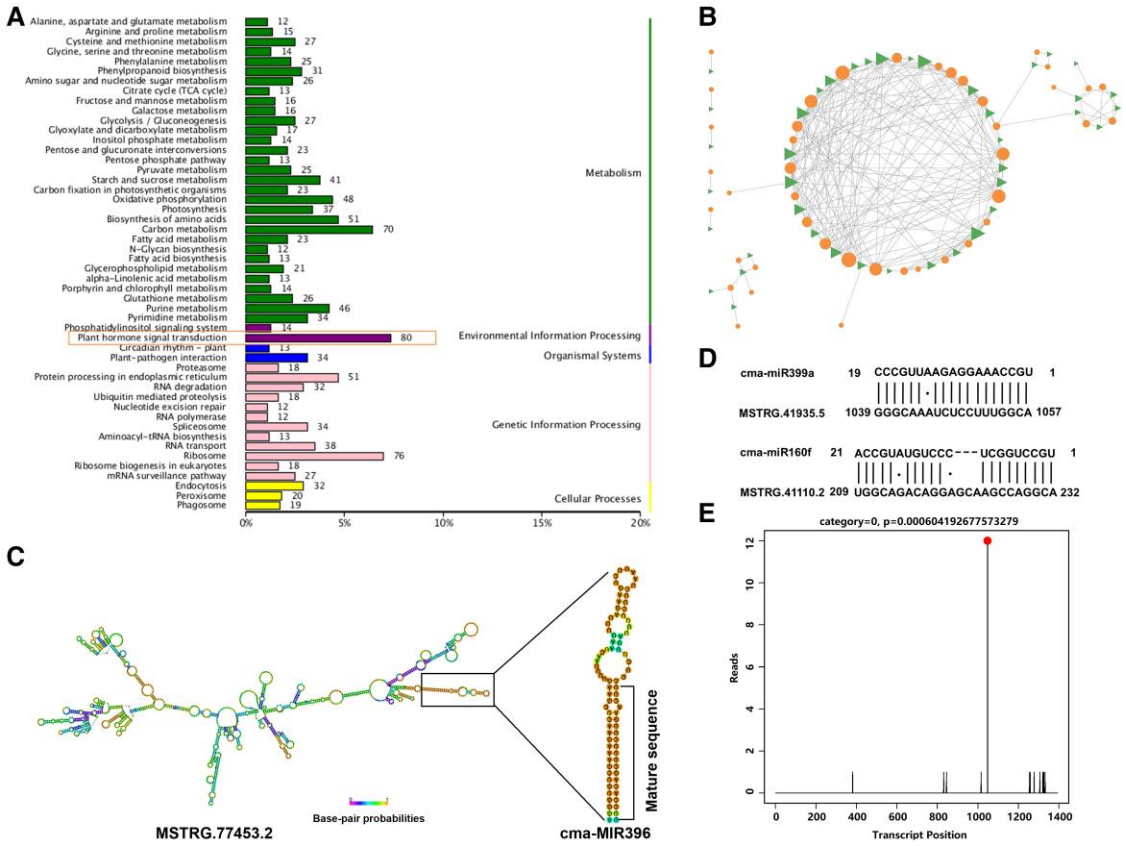

Figure 3. Prediction of target genes and microRNAs interacting with DELs. **A)** Pathway analysis for the potential target genes of DELs. The numbers next to the rectangle represent the number of potential target genes in each pathway. The hollow rectangle marks the pathway that contains the largest number of annotated genes. **B)** Potential regulation network of DELs and target genes involved in plant hormone signal transduction pathway. The circles represent lncRNAs, while the triangles represent potential target genes. **C)** MSTRG.77453.2 was predicted to be a potential precursor of cma-miR396. **D)** MSTRG.41935.5 was predicted as a potential target of cma-miR399a. MSTRG.41110.2 was predicted as a target mimic of cma-miR160f. **E)** The degradome T-plot of MSTRG.41935.5 showed a single distinct peak at the degradation site.

MSTRG.44863.1 using fluorescence in situ hybridization (FISH) in fruits at 0 DAP, demonstrating primary localization in the nucleus and cytoplasm (Fig. 4B), suggesting a potentially diversified regulatory mode. To investigate the potential biological functions of MSTRG.44863.1 in pumpkin, the expression pattern of MSTRG.44863.1 was determined in 11 different tissues of *C. maxima* "Rimu" (Fig. 4C). Using the relative expression level in the apex as the standard, the highest expression was detected in young fruits with lower expression detected in the remaining tissues. In addition, a decreasing expression trend of MSTRG.44863.1 was found between 0 and 10 DAP; the expression level at 2 DAP was only one-fifth that at 0 DAP (Fig. 4C). These analyses indicated a strong tissue- and period-specific expression pattern for MSTRG.44863.1, providing guidance for further exploration of MSTRG.44863.1 functions.

Functional analysis of MSTRG.44863.1

To study the potential role of MSTRG.44863.1 in pumpkin fruit development, we established pumpkin fruit with transient overexpression of MSTRG.44863.1 (MSTRG.44863.1-OE) via *Agrobacterium* injection (Fig. 5A). The expression level of MSTRG.44863.1 was detected at 4 d following the infiltration and a higher expression level in MSTRG.44863.1-OE compared with the empty-vector control fruits (EV-OE) was confirmed by RT-qPCR (Fig. 5B).

RNA-seq using EV-OE and MSTRG.44863.1-OE fruits identified 323 differentially expressed genes (DEGs) ($\log_2$ fold change [FC] > 1 or < -1, $P < 0.05$), including 273 upregulated and 50 downregulated DEGs (Fig. 5C, Supplementary Table S10). KEGG pathway analysis indicated that the DEGs were mainly concentrated in 7 pathways, including the plant hormone signal transduction pathway (Supplementary Table S11 and Fig. S6). In addition, a total of 20 families of differentially expressed transcription factors were found, with the majority represented by ethylene responsive factors (ERFs) (Fig. 5D).

Given that the pathway enrichment and transcription factor analyses indicated that MSTRG.44863.1 may play regulatory roles through hormones, we further determined the hormone contents in EV-OE and MSTRG.44863.1-OE transformed fruits (Supplementary Fig. S7). The results showed a significantly increased content of 1-aminocyclopropane

Downloaded from https://academic.oup.com/plphys/article/195/2/940/7615931 by Beijing Academy of Agriculture & Forestry Sciences user on 31 October 2024

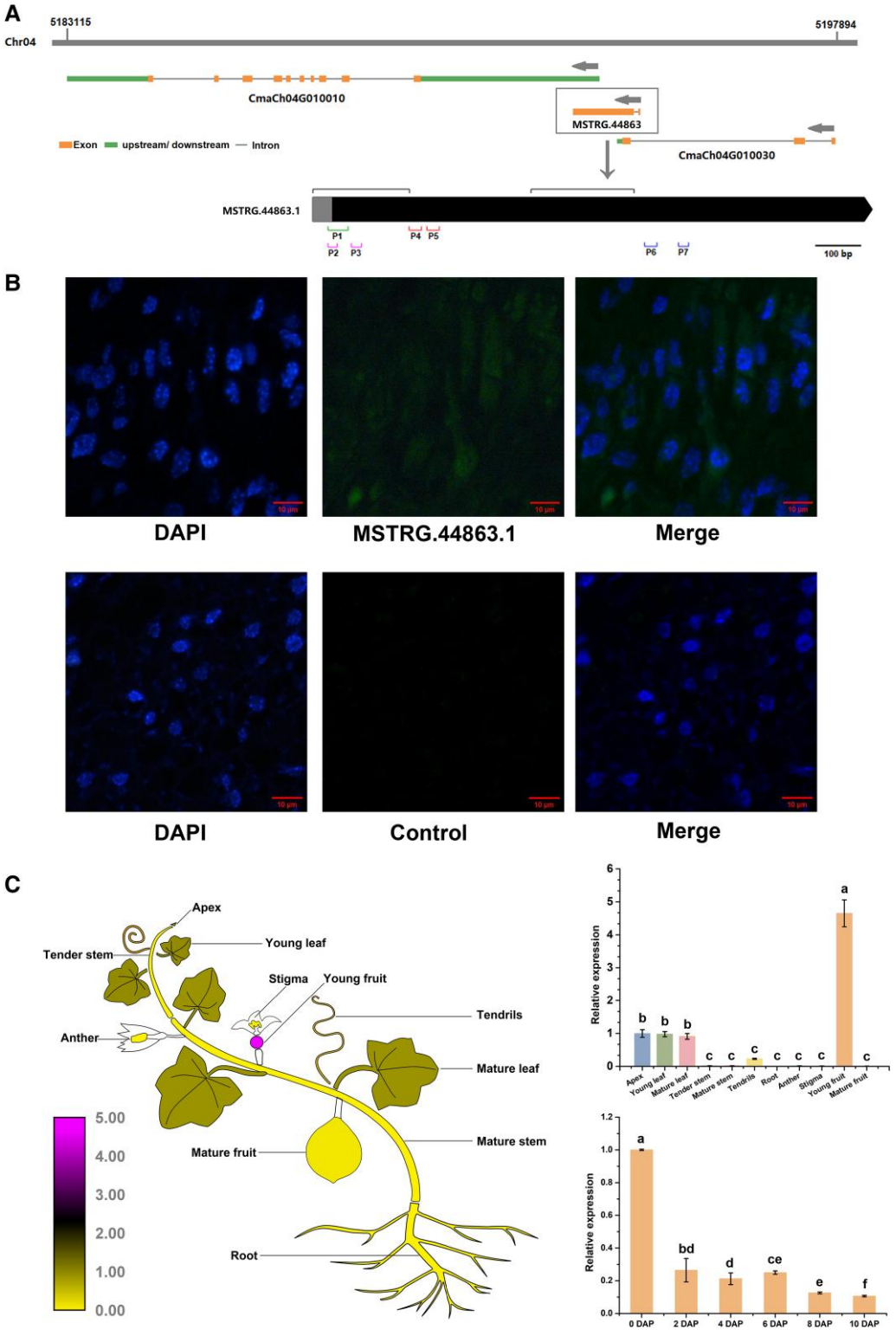

Figure 4. Full-length cloning, localization, and expression analysis of MSTRG.44863.1. **A)** Schematic diagram of the genomic location of MSTRG.44863. The transcription direction is indicated with thick arrows. The gray lines indicate areas where MSTRG.44863.1 does not overlap with any mRNAs. "P1–P7" represent the primers designed for MSTRG.44863.1. "P1" indicates the probe used for *fluorescence* in situ *hybridization*. "P2/P3" indicated the primers used for RT-qPCR. "P5/P4" and "P6/P7" indicate the 5′Race outer/inner primers and 3′Race outer/inner primers, respectively. **B)** Subcellular localization of MSTRG.44863.1 in pumpkin fruit by *fluorescence* in situ *hybridization* using an antisense probe. The FAM-labeled probe was used for detecting MSTRG.44863.1 and a scrambled sequence without a target in pumpkin was used as the negative control. Scale bar, 10 μm. **C)** Expression pattern of MSTRG.44863.1 in different pumpkin tissues and different developmental stages of the fruit, determined by RT-qPCR. Error bars indicate SDS among 3 biological replicates ($n = 3$). Different letters above the bars indicate significantly different values ($P < 0.05$), calculated using ANOVA followed by a Tukey's HSD post hoc test.

Downloaded from https://academic.oup.com/plphys/article/195/2/940/7615931 by Beijing Academy of Agriculture & Forestry Sciences user on 31 October 2024

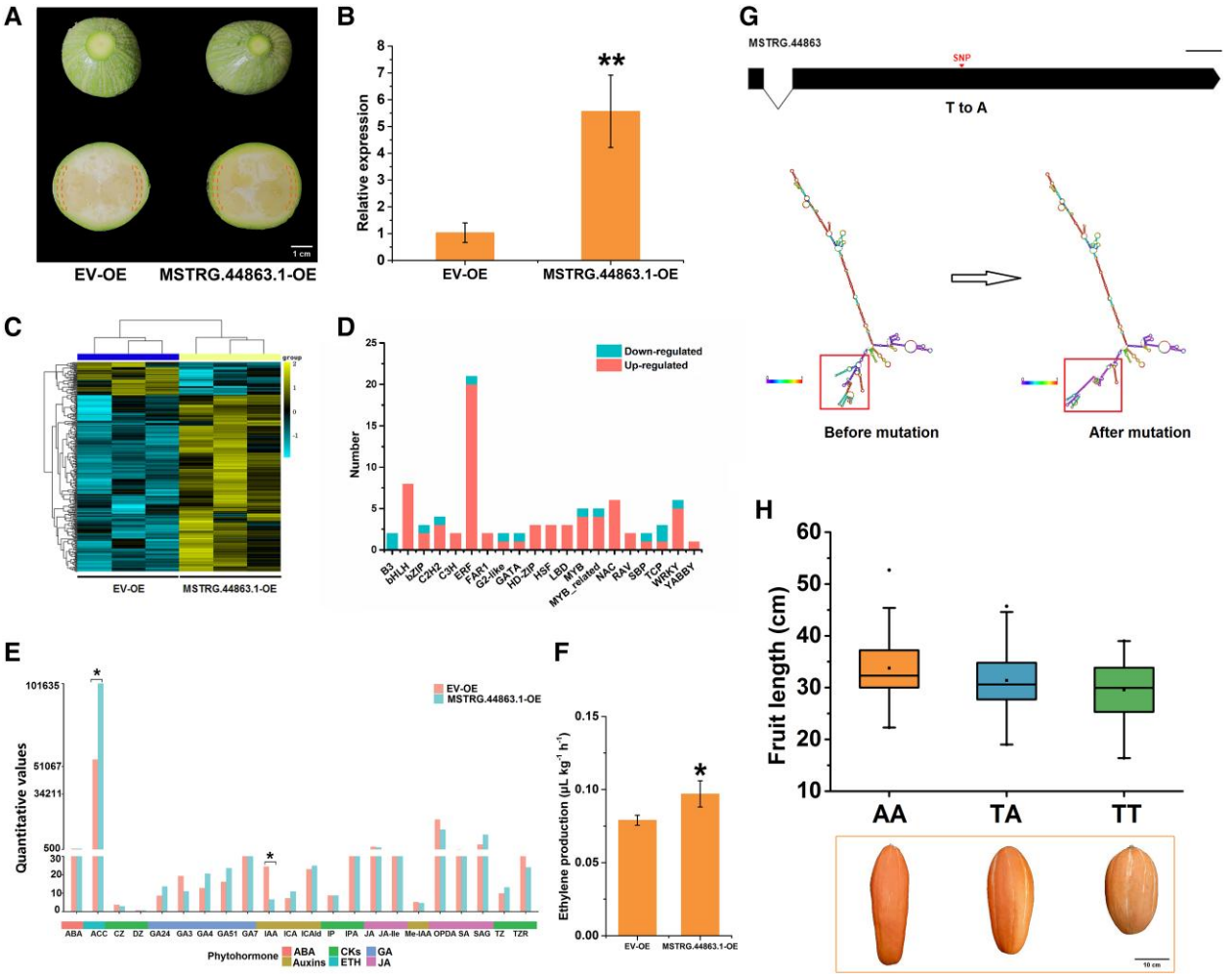

Figure 5. Functional analysis of MSTRG.44863.1. **A)** Transient overexpression of MSTRG.44863.1 in pumpkin fruits; EV, empty vector. Pumpkins were digitally extracted for comparison. **B)** The expression levels of MSTRG.44863.1 in EV-OE and MSTRG.44863.1-OE fruits. Error bars indicate SDs among 3 biological replicates ($n = 3$). Asterisks indicate significant differences between EV-OE and MSTRG.44863.1-OE fruits (**$P < 0.01$) calculated using paired Student's t-test. **C)** Transcriptome expression heatmap of DEGs between MSTRG.44863.1-OE and EV-OE fruits. **D)** Number of downregulated and upregulated transcription factor genes. **E)** Content of different plant hormones in EV-OE and MSTRG.44863.1-OE fruits. Asterisks indicate significant differences between EV-OE and MSTRG.44863.1-OE fruits (*$P < 0.05$) calculated using paired Student's t-test. ABA, abscisic acid; ACC, 1-aminocyclopropane-1-carboxylic acid; CZ, cis-zeatin; DZ, DL-dihydrozeatin; GA, gibberellin; IAA, indole-3-acetic acid; ICA, 3-indoleformic acid; ICAId, indole-3-carboxaldehyde; IP, N6-(delta 2-isopentenyl)-adenine; IPA, N6-isopentenyladenosine-D6; JA, jasmonate acid; JA-IIe, N-[(-)-jasmonoyl]-(S)-isoleucine; Me-IAA, methyl 2-(1*H*-indol-3-yl)acetate; OPDA, 12-oxophytodienoic acid; SA, salicylic acid; SAG, salicylic acid 2-O-β-D-glucose; TZ, trans-zeatin; TZR, trans-zeatin riboside. **F)** Ethylene production in EV-OE and MSTRG.44863.1-OE fruits. Error bars indicate SDs among 3 biological replicates ($n = 3$). Asterisks indicate significant differences between EV-OE and MSTRG.44863.1-OE fruits (*$P < 0.05$) calculated using paired Student's t-test. **G and H)** One SNP within MSTRG.44863.1, a mutation that may result in the secondary structure change, was associated with fruit length ($P < 0.05$) calculated using ANOVA (AA: 45, TA: 76, TT: 40, genotype missing: 3). Pumpkin fruits were digitally extracted for comparison. Central lines are medians, and box limits are the first and third quartiles. The squares in the box represent the average values. Whiskers mark the minimal (lower whisker) and maximal (upper whisker) data points within 1.5 times the interquartile range from the first and third quartiles, respectively. The points represent outliers.

carboxylic acid (ACC), a precursor of ethylene, and a significantly decreased IAA content in MSTRG.44863.1-OE fruit compared with in the control fruit (Fig. 5E). In addition, the MSTRG.44863.1-OE fruit exhibited significantly increased ethylene production compared with that in the control fruit (Fig. 5F).

We also established pumpkin fruits with transient silenced expression of MSTRG.44863.1 using RNA interference (RNAi) (Supplementary Fig. S8A). RT-qPCR analysis confirmed the lower relative expression level of MSTRG.44863.1 in MSTRG.44863.1-RNAi pumpkin fruits (Supplementary Fig. S8B). Considering that transient overexpression of MSTRG.44863.1 significantly affected the levels of ACC, IAA, and ethylene, we further determined these indicators in EV-RNAi and MSTRG.44863.1-RNAi pumpkin fruits (Supplementary Fig. S8, C to E). The results showed that the

Downloaded from https://academic.oup.com/plphys/article/195/2/940/7615931 by Beijing Academy of Agriculture & Forestry Sciences user on 31 October 2024

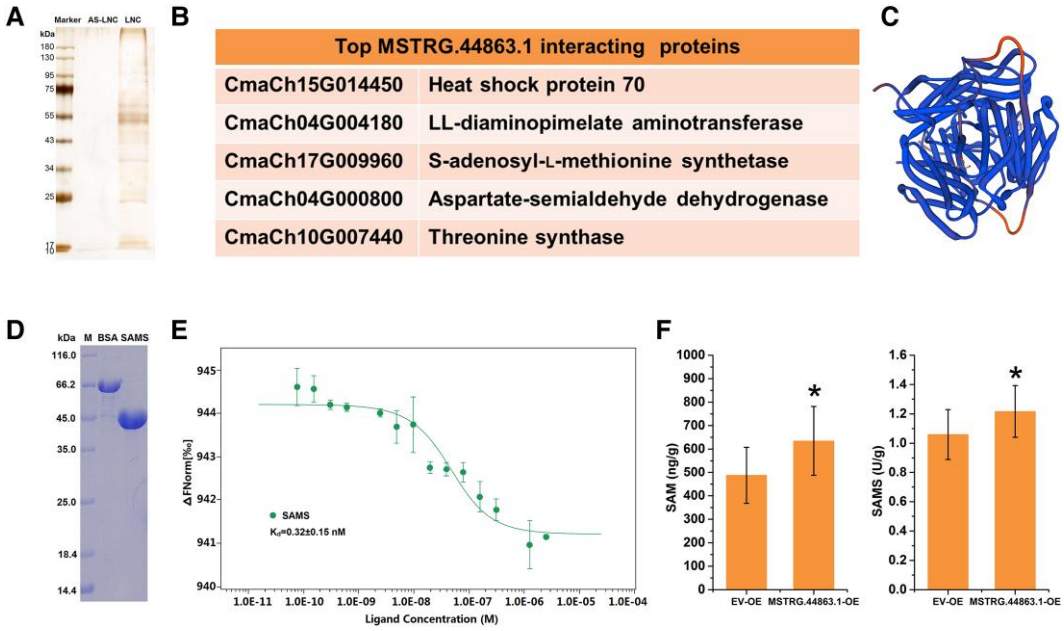

Figure 6. MSTRG.44863.1 interacts with SAMS. **A and B)** Interaction between MSTRG.44863.1 and SAMS was demonstrated by in vitro RNA pull-down assay. **A)** Silver staining following RNA pull-down of MSTRG.44863.1 sense (LNC) or MSTRG.44863.1 antisense (AS-LNC). **B)** Five top candidates for MSTRG.44863.1-interacted proteins identified by mass spectrometry analyses. **C)** Structure prediction of SAMS. **D)** Heterologous expression of SAMS. M, marker; BSA, bovine serum albumin; SAMS, *S*-adenosyl-L-methionine synthetase. **E)** MST indicating the binding of MSTRG.44863.1 to SAMS. **F)** The content of SAM and activity of SAMS are upregulated in MSTRG.44863.1-OE pumpkin fruit compared with in EV-OE pumpkin fruit. Error bars indicate SDS among 3 biological replicates ($n = 3$). Asterisks indicate significant differences between EV-OE and MSTRG.44863.1-OE fruits ($^*P < 0.05$) calculated using paired Student's *t*-test.

ACC content and ethylene production were significantly decreased, while the IAA content was markedly increased in the MSTRG.44863.1-RNAi fruit compared with in the control fruit.

Population genomic analysis of MSTRG.44863.1

To further study the effect of MSTRG.44863.1 on fruit development, we dissected the allelic variation in MSTRG.44863 underlying fruit-related characteristics using single-nucleotide polymorphism (SNP)-based association analysis. Using a previously constructed population of 164 F_2 *C. maxima* individuals, we found a SNP (Cma_Chr04-5193631) in the genomic sequence of MSTRG.44863 between the 2 parental lines. Secondary structure prediction indicated that this SNP may alter the predicted structure of MSTRG.44863.1 (Fig. 5G). Analysis of variance (ANOVA) confirmed significant differences ($P < 0.05$) between the fruit length corresponding to the 3 genotypes of this SNP (Fig. 5H). Considering that previous studies in cucurbits have linked ethylene to fruit length, our results indicated that MSTRG.44863.1 may affect fruit length by modulating ethylene synthesis. The genotype and phenotype data are provided in Supplementary Table S12.

Dissection of the regulatory mechanism of MSTRG.44863.1

To further investigate the regulatory mechanism of MSTRG.44863.1, an in vitro RNA pull-down assay was carried out and the protein interactome of MSTRG.44863.1 was filtered by mass spectrometry (Fig. 6A). The sense and antisense strands of MSTRG.44863.1 were amplified to obtain templates for in vitro transcription (Supplementary Fig. S9). The potential target proteins of MSTRG.44863.1 are provided in Supplementary Table S13. The top 5 unique proteins (unused ≥ 5, peptides ≥ 3) specifically interacting with the biotin-labeled sense group but not the control antisense group are shown in Fig. 6B. Among them, SAMS (Fig. 6C) was associated with the function of MSTRG.44863.1. SAMS catalyzes methionine and ATP to generate *S*-adenosyl-L-methionine (SAM), which is involved in ethylene biosynthesis via ACC. Therefore, SAMS was hypothesized to be a target of MSTRG.44863.1.

We further verified the possible direct interaction between MSTRG.44863.1 and SAMS using a microscale thermophoresis (MST) assay (Supplementary Fig. S10), which facilitates sensitive measurements of molecular interactions in solution. The SAMS protein was obtained by a prokaryotic expression system (Fig. 6D). The MST results showed that MSTRG.44863.1 bound to SAMS at low micromolar concentrations of the titrant, exhibiting a dissociation constant (K_d) of 0.32 ± 0.15 nM (Fig. 6E), suggesting a relatively strong interaction. Moreover, transient overexpression and silencing of MSTRG.44863.1 affected the SAM content and SAMS activity (Fig. 6F, Supplementary Fig. S11). Specifically, the SAM content and SAMS protein level were significantly increased in the fruit with MSTRG.44863.1-OE relative to in the fruit

Downloaded from https://academic.oup.com/plphys/article/195/2/940/7615931 by Beijing Academy of Agriculture & Forestry Sciences user on 31 October 2024

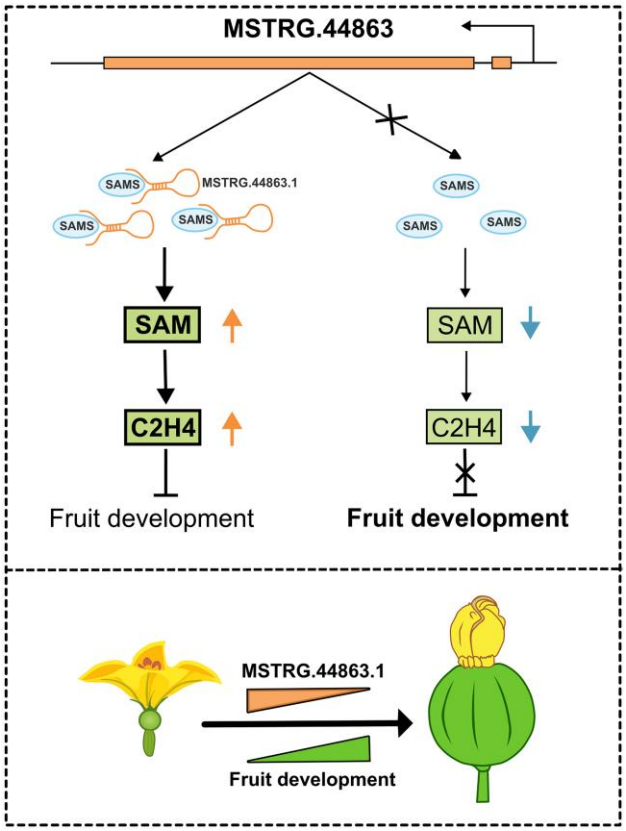

Figure 7. Proposed model for the regulation mechanism of MSTRG.44863.1 on pumpkin fruit development via interacting with SAMS. When the expression of MSTRG.44863.1 is high, MSTRG.44863.1 binds to SAMS and promotes the synthesis of SAM, which in turn increases the ethylene (C_2H_4) content; the high ethylene concentrations ultimately inhibit fruit development. When MSTRG.44863.1 shows low or no expression, SAM synthesis is reduced, which leads to lower ethylene content. As the low concentrations of ethylene cannot sustain the inhibition of fruit development, the fruit begins to develop. Therefore, MSTRG.44863.1 and fruit development are negatively associated. The arrows indicate positive regulation, and blunt-ended bars indicate inhibition. The turning arrow represents the transcription direction. The crosses represent the release of positive regulation/inhibition. An upward arrow next to SAM/C2H4 represents an increase in content, while a downward arrow in next to SAM/C2H4 represents a decrease in content.

with EV-OE (Fig. 6F). These results indicated that MSTRG.44863.1 potentially interacts with SAMS. Finally, we proposed a model where MSTRG.44863.1 regulates pumpkin fruit development by interacting with SAMS (Fig. 7).

Discussion

Establishment of an lncRNA dataset related to fruit development in *C. maxima*

Cucurbits are a large and diverse plant family that supplies many important fruits. Among this family, pumpkin is a preferred model for understanding the molecular mechanisms regulating fruit development owing to its variable shape and size and large inferior ovary. Recently, lncRNAs have been identified as important regulatory molecules (Waseem et al. 2020); however, they remain poorly studied in cucurbits, with essentially no information available on lncRNAs in pumpkin fruit. Because of the low conservation of lncRNAs across species (Wu et al. 2020), it is hard to predict the function of lncRNAs based only on their sequence similarity to known lncRNAs. Therefore, it is necessary to identify and characterize species-specific lncRNAs.

In this study, we identified lncRNAs in pumpkin (*C. maxima*) based on genome-wide analysis, including a total of 5,425 lncRNAs expressed throughout the fruit development. Four computational methods were used to sort ncRNA candidates from protein-coding RNAs and only transcripts with more than 2 exons were selected as lncRNA candidates. These measures effectively reduced the false positives of lncRNA prediction. Since previous reports showed that lncRNAs have high specificity in various tissues and stages of development, we selected 6 different sampling points throughout the fruit development to obtain more complete information. As expected, most of the identified lncRNAs were period-specific, with only a quarter of the lncRNAs identified in all the 6 developmental stages.

The identified lncRNAs of *C. maxima* shared similar characteristics with the lncRNAs of other species. Previous studies have shown that lncRNAs are shorter with lower expression levels than mRNAs (Pauli et al. 2012; Li et al. 2014, 2022a; Wang et al. 2014; Hao et al. 2015; Gao et al. 2020), including studies from *Arabidopsis* (Liu et al. 2012; Wang et al. 2014), cucumber (Hao et al. 2015), and melon (Gao et al. 2020). Consistently, we found that the mean length of *C. maxima* lncRNAs is less than half that of *C. maxima* mRNAs, and their expression levels were significantly lower than those of mRNAs (Fig. 1, E and F). However, the low expression of lncRNAs can make a big difference in many biological processes. Moreover, most lncRNA sequences exhibit weak conservation among species (Deng et al. 2018), such as the lncRNAs in Chinese cabbage (*Brassica rapa* ssp. *pekinensis*) (Song et al. 2021). The present BLAST analyses showed most (99.10%) of the identified lncRNAs are likely pumpkin-specific. These results suggest that lncRNAs in pumpkin are rapidly evolving, similar to those of other plants. In addition, the genome positions of *C. maxima* lncRNAs are distributed across all the 20 chromosomes. Such widespread chromosomal distribution has been reported in lncRNAs of other plants (Hao et al. 2015; Tian et al. 2022), suggesting that lncRNAs constitute an important functional part of the genome.

To identify lncRNAs related to fruit development, we identified 322 DELs as important candidates for further investigation of the regulatory mechanisms of fruit development. Previous research has shown that miRNAs, lncRNAs, and mRNAs may exhibit crosstalk (Jiang et al. 2019; Lucero et al. 2021; Tang et al. 2021). The present results also indicated that lncRNAs may interact with genes or miRNAs (Fig. 3), which may be helpful for further DEL function research. Overall, these findings improve our understanding of fruit-related lncRNAs and provide a rich resource for their further study.

Downloaded from https://academic.oup.com/plphys/article/195/2/940/7615931 by Beijing Academy of Agriculture & Forestry Sciences user on 31 October 2024

Regulation of MSTRG.44863.1 in pumpkin fruit development

Owing to the low level of expression and the complex function of lncRNAs in plants, knowledge of their specific functions remains limited. Previous studies confirmed the important roles of lncRNAs in fruit development. However, the function of lncRNAs during fruit development in cucurbits has not yet been elucidated. In this study, we found that the lncRNA MSTRG.44863.1 was highly expressed at 0 DAP, and then its expression continued to decline with almost no expression detected after 10 DAP (Fig. 4C). The relatively high expression level and obvious period-specific expression pattern suggests the importance of MSTRG.44863.1 in fruit development.

RNA-seq of pumpkin fruit with transient overexpression of MSTRG.44863.1 showed the concomitant upregulation of ethylene synthesis-related genes and ERFs (Supplementary Table S10, Fig. 5, B to D). In addition, overexpression of MSTRG.44863.1 increased the content of ACC, a precursor of ethylene (Fig. 5E). The transient overexpression and silencing of MSTRG.44863.1 significantly affected ethylene production (Fig. 5F, Supplementary Fig. S8E). Taken together, these results indicated that MSTRG.44863.1 is positively associated with ethylene synthesis. Previous studies indicated a negative correlation between the production of ethylene in the ovary and fruit set and early fruit growth (Martínez et al. 2013; Shinozaki et al. 2015). Transcriptome studies in tomato showed a decrease in the transcript levels of genes encoding proteins involved in ethylene biosynthesis and signaling in early fruit development (Vriezen et al. 2008; Wang et al. 2009). Furthermore, ethylene was reported to inhibit tomato fruit setting through modification of the gibberellin metabolism (Shinozaki et al. 2015). The application of high concentrations of ACC to pollinated ovaries can lead to smaller tomato fruits, indicating that ethylene has a negative effect on fruit growth (Shinozaki et al. 2015). Ovarian ethylene in the days immediately after anthesis plays an important role as a negative regulator of fruit set and early fruit development in zucchini (Martínez et al. 2013). Pollination/fertilization induces fruit set and development by preventing the production and action of ethylene immediately after anthesis. Therefore, we propose a mechanism by which MSTRG.44863.1 negatively regulates fruit development by influencing ethylene synthesis (Fig. 7).

In various fruit crops, auxin negatively regulates ethylene after fertilization. Evidence from tomatoes suggests that auxin negatively regulates the production of ethylene in the early fruit through transcriptional regulation (Shinozaki et al. 2015). Consistently, auxin-dependent inhibition of ethylene production and associated gene expression were observed in the early development of zucchini fruit (Martínez et al. 2013). This raises the question of whether lncRNAs are involved in the crosstalk between auxin and ethylene in fruit development. In this study, we found that MSTRG.44863.1 expression was downregulated 4 h after IAA (100 mg/L) application (Supplementary Fig. S12). In addition, the IAA content was significantly reduced in the MSTRG.44863.1-OE fruits compared with that of the control (Fig. 5E), while the content of ACC and ethylene production increased significantly (Fig. 5, E and F). Taken together, these results suggested that MSTRG.44863.1 may participate in the crosstalk between auxin and ethylene in pumpkin fruit development. We suspect that auxin in the ovary may reduce the biosynthesis of ethylene after pollination/fertilization, by decreasing the expression of MSTRG.44863.1.

Previous studies demonstrated that ethylene can affect fruit length in cucurbits (Xin et al. 2019; Boualem et al. 2022). In cucumber, mutants that produce more or less ethylene showed fewer cell divisions and shorter fruits than the wild type (Xin et al. 2019). Based on the abovementioned association between MSTRG.44863.1 and ethylene synthesis, we conducted SNP-based association analysis to explore the effects of MSTRG.44863.1 on fruit length. We found an SNP mutation in the genomic sequence of MSTRG.44863 associated with fruit length (Fig. 5, G and H). Further analysis showed that this SNP may affect the secondary structure of MSTRG.44863.1, suggesting an impact on its regulatory function to influence the final fruit phenotype. Studies suggested that ethylene had a dose-dependent effect on the development of cucumber fruit and a bidirectional regulating effect of fruit size in tomato (Liu et al. 2014; Sharma et al. 2021; Huang et al. 2022). However, the potential bidirectional regulatory effect of ethylene on pumpkin fruit development requires further exploration. Since the gene sequence of MSTRG.44863 is conserved among *Cucurbita* species, it is speculated that its function in fruit development may also be conserved within the genus, although this requires validation. Collectively, these results advance our understanding of the function of lncRNAs in fruit development, indicating a key role in the fine-tuning of ethylene production in different tissues at various critical stages of development.

Molecular mechanism of MSTRG.44863.1 regulating fruit development

We identified that MSTRG.44863.1 can regulate hormone contents during pumpkin fruit development, confirming its important role in fruit development. However, the molecular mechanism underlying this hormone regulation needs to be further elucidated.

Recent studies have found that lncRNAs can function via various complex mechanisms, including interacting with miRNAs, affecting the expression of adjacent genes, and binding to proteins. Using bioinformatics prediction, we first ruled out the possibility that MSTRG.44863.1 interacts with miRNAs. In addition, there was no obvious co-expression trend between MSTRG.44863.1 and its neighboring genes during pumpkin fruit development. According to these results, we finally speculated that MSTRG.44863.1 may regulate fruit development by interacting with proteins. Previous studies demonstrated that protein interaction is the key

Downloaded from https://academic.oup.com/plphys/article/195/2/940/7615931 by Beijing Academy of Agriculture & Forestry Sciences user on 31 October 2024

mechanism of action of lncRNAs. For example, the lncRNA highly upregulated in liver cancer was reported to promote aerobic glycolysis through direct binding with lactate dehydrogenase A and pyruvate kinase M2 (Wang et al. 2020a). In maize (*Zea mays*), it was reported that lncRNA GARR2 may interact with the homologous to the E6-AP carboxyl terminus ubiquitin–protein ligase family member ZmUPL1 to modulate gibberellin response (Li et al. 2022b). Another study showed that BPA1-LIKE PROTEIN3 (BPL3) of *Arabidopsis* directly binds to the lncRNA nalncFL7 to coordinate plant immunity (Ai et al. 2023). The results of our RNA pull-down and MST assays suggested that SAMS may be a protein target of MSTRG.44863.1 (Fig. 6).

In plants, ethylene is synthesized from methionine via the intermediates SAM and ACC, and ethylene biosynthesis can be regulated at both the gene expression and protein activity levels (Bouvier et al. 2006). The biosynthesis of ethylene depends on a stable supply of SAM, which is produced from methionine by SAMS (also called methionine adenosyltransferase). Our results suggest that the interaction between MSTRG.44863.1 and SAMS is responsible for the observed altered ACC content and ethylene production upon transient overexpression and silencing of MSTRG.44863.1. In *Arabidopsis*, *S*-adenosyl-L-methionine synthetase 4 (METK4) can bind to RNA in the leaf, which was further verified by an independent plant RNA interactome capture (ptRIC) test followed by proteomic or western blotting analysis (Bach-Pages et al. 2020), suggesting that SAMS is an RNA-binding protein. Previous studies clarified that post-translational modifications of SAMS lead to altered ethylene levels, suggesting that SAM homeostasis is closely related to ethylene biosynthesis. However, the specific mode of interaction between MSTRG.44863.1 and SAMS in pumpkins remains to be further explored. In addition to its role in ethylene biosynthesis, SAM is also involved in the biosynthesis of polyamines, which play important roles in plant growth, development, and stress responses (Chen et al. 2019). It is also a universal methyl group donor involved in numerous transmethylation reactions (Rocha et al. 2005; Zhang et al. 2011; Lindermayr et al. 2020). Therefore, the expression of MSTRG.44863.1 in multiple tissues may be related to the involvement of SAM in diverse biological pathways.

In summary, our results suggest that the lncRNA MSTRG.44863.1 interacts with SAMS, which affects ethylene synthesis, leading to the negative regulation of pumpkin fruit development (Fig. 7). These results provide insights into the regulatory mechanisms of fruit development.

Materials and methods

Plant materials and growth conditions

The pumpkin (*C. maxima*) material used in this study was derived from the highly inbred line "Rimu" with a complete genome sequence available (Sun et al. 2017). *C. maxima* "Rimu" plants were grown under natural light conditions in a greenhouse at the farm of Beijing Vegetable Research Center, Beijing, China (39°56′40.8″N, 116°15′55.4″E) under standard agronomic conditions. Fruit pulp was collected at 0, 10, 20, 30, 40, and 50 DAP, with 3 biological replicates per time point. All harvested samples were immediately frozen in liquid nitrogen after collection and stored at −80 °C until use.

Measurement of fruit-related characteristics

Nine fruit-related characteristics were measured using the fruit pulp of "Rimu" with 3 biological replicates for assessment of each trait per time point: fruit length, fruit diameter, pulp thickness, lutein content, β-carotene content, sucrose content, glucose content, fructose content, and starch content. Fruit length, fruit diameter, and pulp thickness were measured using a digital Vernier caliper. A longitudinal section of each pumpkin fruit was used to measure the length, diameter, and thickness of the fruit.

The contents of carotenoid, sugar, and starch were determined with freeze-dried samples. Carotenoids including lutein and β-carotene were measured with high-performance liquid chromatography (HPLC), as described by Zhong et al. (2011). The carotenoid content was measured at 450 nm and determined by comparison of retention times and spectra with known standards. The contents of sucrose, glucose, and fructose in the fruit flesh were also determined by HPLC following the methods described by Zhong et al. (2017). The sugars were quantified by comparison with standards purchased from Sigma. Starch was isolated and analyzed following the method of Stevenson et al. (2005).

RNA isolation, library construction, and sequencing

We used fruit pulp collected at the 6 DAP time points (3 biological replicates per time point) for high-throughput RNA-seq. Total RNA was extracted using a Qiagen RNAeasy kit (Qiagen China, Shanghai, China) according to the manufacturer's instructions. Genomic DNA was removed by treatment with RNase-Free DNase Set (Qiagen). The quality and integrity of RNA were checked after observation on a 1.5% agarose gel. After removal of ribosomal RNA using Ribo-Zero rRNA Removal Kit (Epicentre, Madison, WI, USA), the sequencing libraries was generated using a NEBNextR Ultra Directional RNA Library Prep Kit for Illumina (New England Biolabs, Ipswich, MA, USA). Finally, 18 strand-specific RNA-seq libraries were generated and sequenced on a HiSeq 4000 system (Illumina Inc., San Diego, CA, USA) according to the manufacturer instructions.

Read mapping, identification, and characterization of lncRNAs

The quality of the raw sequencing data was checked with FASTQC. Clean data were obtained by deleting reads containing adapters and poly-N along with low-quality reads from the raw data. The remaining clean reads were mapped to the *C. maxima* ("Rimu") genome (version 1.1) (Sun et al. 2017) using HISAT (Kim et al. 2015). The transcriptome was assembled using StringTie v1.3.1 (Pertea et al. 2016) based on the reads mapped to the reference genome. The

Downloaded from https://academic.oup.com/plphys/article/195/2/940/7615931 by Beijing Academy of Agriculture & Forestry Sciences user on 31 October 2024

assembled transcripts were annotated using the gffcompare program.

Based on RNA-seq data, lncRNAs were predicted in accordance with Sun et al. (2013) using a series of strict screening pipelines, as shown in Supplementary Fig. S13. Transcripts with mapping coverage less than half the transcript length and transcripts with fragments per kilobase of transcript per million mapped reads (FPKM) < 0.1 were removed. Transcripts with a length > 200 nucleotides and with over 2 exons were selected as lncRNA candidates for further evaluation of coding potential. Four computational approaches, Coding Potential Calculator, Coding–NonCoding Index, Coding Potential Assessment Tool, and Pfam-scan (Pfam), were combined to sort nonprotein coding RNA candidates from putative protein-coding RNAs in the unknown transcripts. According to their genomic locations, the final determined lncRNAs were classified into 4 types: lincRNAs, intronic lncRNAs, antisense lncRNAs, and sense lncRNAs (Roberts et al. 2011).

A BLAST search was performed on all the lncRNA sequences identified against known lncRNAs of other plant species in the GREENC (Gallart et al. 2016) and CANTATAdb (Szcześniak et al. 2016) databases using BLASTN (coverage > 80% and *E*-value < 1e−10). Repeat Masker was used to analyze the content of repetitive elements in the identified lncRNAs. The GC content of the identified lncRNAs was calculated using the EMBOSS Explorer *geecee* tool. The software and analyzed website information are shown in Supplementary Table S14.

Analysis of differential expression patterns

Expression levels of the assembled transcripts were calculated and normalized using Fragments Per Kilobase of transcript per Million mapped reads (FPKM) by StringTie v1.3.1 (Pertea et al. 2016). The DESeq R package v1.10.1 was for the differential expression analysis of 2 groups. A positive false discovery rate (Storey 2002) was used to adjust the obtained *P* values. Only the lncRNAs that met the criteria of $\log_2$FC ≥1 or ≤−1 with an adjusted *P* value < 0.05 were assigned as DELs.

Target gene prediction of lncRNAs and functional enrichment analysis

The potential target genes of lncRNAs were predicted according to their regulatory mode: cis- and trans-acting. Prediction of cis target genes was mainly based on the position relationship between the lncRNA and the gene. Genes that were transcribed within 100 kb upstream or downstream of the lncRNAs were considered to be cis target genes (Jia et al. 2010). Based on the sequence complementarity and standardized free energy, the software LncTar (Li et al. 2015) was used to predict trans-acting target genes of lncRNAs, with normalized free energy <−0.1. Using topGO R packages, GO enrichment analysis of target genes was performed, with an adjusted *P* value < 0.05. The KOBAS (Xie et al. 2011) software was used for pathway enrichment and Cytoscape 3.2.0 was used to generate the co-expression network.

Prediction of interactions with miRNAs and degradome analysis

LncRNAs as precursors of miRNAs were predicted by aligning the mature miRNA sequences to the putative lncRNA sequences, with no mismatch permitted. LncRNAs as potential targets of miRNAs were predicted by psRNATarget (Dai and Zhao 2011) with expectation ≤ 5. The target mimics were predicted according to the criteria proposed by Wu et al. (2013). The secondary structures of lncRNAs and miRNAs were predicted using the Vienna RNA package in the RNAfold web server. The details of the bioinformatic software used are listed in Supplementary Table S14. For degradome analysis, RNAs from 18 fruit samples were pooled for the degradation library construction and then sequenced using the Illumina HiSeq 2500 platform (LC Sciences, Hangzhou, China).

RT-qPCR

Total RNA was extracted using a Qiagen RNAeasy kit (Qiagen China) according to the manufacturer instructions and then reverse-transcribed with the lnRcute lncRNA First-Strand cDNA Synthesis Kit (Tiangen, China). The qPCR was carried out on an ABI7500 system (Thermo Fisher Scientific, Waltham, MA, USA) using the lnRcute lncRNA qPCR Detection Kit (Tiangen). Amplification was performed in triplicate with the standard reaction program. Relative gene expression levels were normalized to *ACTIN* (CmaCh11G016220) and calculated using the $2^{-\Delta\Delta Ct}$ method (Livak and Schmittgen 2001). The primers used for RT-qPCR are listed in Supplementary Table S15.

RACE

The 5′ and 3′ ends of MSTRG.44863.1 were obtained using a 5′ RACE System (Invitrogen) and a 3′-Full RACE Core Set (TaKaRa) according to the manufacturers' instructions. Primers used to amplify 5′ and 3′ sequences were designed based on the RNA-seq sequence of MSTRG.44863.1. The amplified fragment was finally determined by Sanger sequencing. The RACE primers are listed in Supplementary Table S15.

RNA FISH

The subcellular localization of MSTRG.44863.1 was examined using FISH. The fruits at 0 DAP were cut into small pieces, immersed in formalin-aceto-alcohol fixative solution (Gefan Biotech, Shanghai, China) for over 24 h, and embedded in paraffin blocks after ethanol dehydration at room temperature. The FAM (fluorescein)-labeled probe was used for detecting MSTRG.44863.1, and a scrambled sequence without a target in pumpkin was used as the negative control. All probes were synthesized by GenePharma (Shanghai, China) (Supplementary Table S15). The fluorescent signals of the detected samples were observed with a Nikon Eclipse Ci confocal microscope. For probes labeled with FAM, an excitation line of 488 nm was applied and

Downloaded from https://academic.oup.com/plphys/article/195/2/940/7615931 by Beijing Academy of Agriculture & Forestry Sciences user on 31 October 2024

signals were detected at 500 to 550 nm; for observing DAPI (4′,6-diamidino-2-phenylindole) nuclear staining, an excitation line of 405 nm was applied and signals were detected at 420 to 480 nm. The laser intensity was set to 6% for 405 nm and 4% for 488 nm. The analog gain was set to 2.8 for 405 nm and 5.1 for 488 nm.

Transient expression of MSTRG.44863.1 in pumpkin fruits

The vector pCAMBIA2301 was used to overexpress and silence MSTRG.44863.1. The full-length MSTRG.44863.1 sequence was amplified from the cDNA of pumpkin fruits and recombined into the pCAMBIA2301 vector. To construct the FaAKR23-RNAi vector, the forward and reverse fragments near the 5′ end of MSTRG.44863.1 were amplified, and the intron fragment was amplified using the PBSK-RTM plasmid as the template. The 3 amplified fragments were then inserted into the pCAMBIA2301 plasmid by a seamless cloning method. MSTRG.44863.1-OE, MSTRG.44863.1-RNAi, and empty vectors as controls (EV-OE and EV-RNAi) were introduced into the *Agrobacterium tumefaciens* strain GV3101 via electroporation and cultured in Luria–Bertani medium at 28 °C. The transient overexpression vectors were sequenced for further validation. The *Agrobacterium* culture was resuspended in an infiltration buffer (10 mM MES [pH 5.6], 10 mM $MgCl_2$, 200 μM acetosyringone) and then adjusted to an optical density at 600 nm of 0.3. The *Agrobacterium* suspension (100 μL) was injected into the pumpkin fruits at 0 DAP. Four days later, the injected fruits were collected, frozen in liquid nitrogen, and stored at −80 °C for further analysis. Each transient transformation experiment was repeated at least 3 times. The primers used in vector construction are displayed in Supplementary Table S15.

Transcriptome, phytohormone content measurement, ethylene production, and enzyme-linked immunosorbent assay

The transcriptomes of EV-OE and MSTRG.44863.1-OE pumpkin fruits were sequenced using the Illumina Hiseq2000 platform. Genes with an adjusted P value <0.05 and absolute value of $\log_2FC \geq 1$ were considered differentially expressed.

The phytohormone contents of selected EV-OE and MSTRG.44863.1-OE pumpkin fruits were measured using liquid chromatography–mass spectrometry by PANOMIX Biomedical Tech Co., Ltd. (Suzhou, China). Three biological replicates were analyzed for each line. The ACC and IAA contents of the selected EV-RNAi and MSTRG.44863.1-RNAi pumpkin fruits were measured using the respective plant enzyme-linked immunosorbent assay (ELISA) Kits (Shanghai Ruifan Biological Technology Co., Ltd.) following the manufacturer's protocol. Ethylene production (μL kg^{-1} h^{-1}) was determined using a gas chromatograph (7820, Agilent Technologies Inc., Foster City, CA, USA) according to a method reported by Yan et al. (2020). The experiment was repeated 3 times. Quantification of SAM concentration and SAMS activity was conducted using the respective plant ELISA Kits (Shanghai Ruifan Biological Technology Co., Ltd.) following the manufacturer's protocol.

Association analysis

A population of 164 F_2 *C. maxima* individuals was generated from a single F_1 plant by crossing parental lines characterized by contrasting phenotypes for fruit traits. The F_2 individuals were grown and evaluated using standard horticultural practices, strictly under self-pollination. Each plant should only have one fruit to ensure sufficient nutrition. All self-hybridized fruits were collected at 50 DAP and used for the analysis of fruit-related phenotypes.

The SNP data were obtained from resequencing of the 164 F_2 individuals. Young and healthy leaves were sampled, immediately frozen in liquid nitrogen, and stored at −80 °C for DNA extraction. Paired-end libraries were constructed using the TruSeq Library Construction Kit for each individual and paired-end (150 bp) sequencing was performed using the Illumina HiSeq sequencing platform. Clean data were collected from raw reads by removing reads containing adapters, contiguous undetermined nucleotides (>10%), and of low quality (>50% reads with $Q \leq 5$). The filtered resequencing reads were then mapped to the *C. maxima* ("Rimu") genome (version 1.1) using BWA-MEM version 0.7.10 (Li and Durbin 2009) and the repetitive sequences were removed with SAMTOOLS (Li et al. 2009). To avoid sequencing errors, only sequences with a missing rate <20% and biallelic SNPs were selected for analysis.

RNA pull-down

In vitro transcription and biotin labeling were performed using T7 RNA polymerase (Roche, Basel, Switzerland) and the Biotin RNA Labeling Mix Kit (Roche) according to the manufacturer's instructions. Total protein was extracted from pumpkin fruits at 0 DAP using lysis buffer supplemented with a protease inhibitor cocktail (Sigma) and recombinant RNase inhibitor (Takara). Biotin-labeled sense and antisense MSTRG.44863.1 were incubated with the protein extracted from pumpkin fruits at room temperature for 2 h. The beads–RNA–proteins complex was washed with RIP lysis buffer 5 times. The biotin eluent was added to the beads, followed by mass spectrometry identification (FitGene Biotechnology, China). Proteins absent in the negative control were considered positive candidates.

MST assay

MST assays were carried out to verify the binding of MSTRG.44863.1 and SAMS as described previously (Jerabek-Willemsen et al. 2011). Approximately 16 samples with constant concentrations of fluorescently labeled SAMS and 2-fold increased concentrations of nonlabeled MSTRG.44863.1 were mixed and incubated for 30 min at room temperature. The binding assays were performed with a Monolith NT.115 system (NanoTemper Technologies, Munich, Germany) using standard treated capillaries. In

Downloaded from https://academic.oup.com/plphys/article/195/2/940/7615931 by Beijing Academy of Agriculture & Forestry Sciences user on 31 October 2024

addition, the variation in fluorescence distribution upon heating was measured as a function of the RNA–protein complex concentration. The dissociation constant (K_d) was calculated and fitted using the Nano Temper Analysis software. Three independent measurements were taken.

Statistical analysis

All of the experiments were carried out with 3 biological replicates. Standard deviation (SD) was calculated using the function STDEV in Excel. Two groups of data were compared using paired Student's *t*-test (*$P < 0.05$; **$P < 0.01$). Multiple groups of data were compared using 1-way ANOVA and Tukey's honestly significant difference (HSD) post hoc test with $P < 0.05$ being considered significant.

Accession numbers

The raw sequence data have been uploaded to the Genome Sequence Archive (GSA) in the National Genomics Data Center, Beijing Institute of Genomics, Chinese Academy of Sciences (https://bigd.big.ac.cn/), under accession numbers CRA012641 and CRA012688. Sequence data from this article can be found in the Cucurbit Genomics Database (http://cucurbitgenomics.org/v2) under the following accession numbers: *ACTIN* (CmaCh11G016220) and *SAMS* (CmaCh17G009960).

Acknowledgments

We thank Dr Qing Wang (Institute of Agri-Food Processing and Nutrition, Beijing Academy of Agricultural and Forestry Sciences) for assistance in the determination of ethylene production.

Author contributions

J.T., C.W., and H.L. planned and designed the research. J.T., F.Z., G.Z., and X.L. performed experiments. J.T. analyzed the data. J.T., C.W., and H.L. wrote the manuscript. All authors read and approved the final manuscript.

Supplementary data

The following materials are available in the online version of this article.

Supplementary Figure S1. Phenotypic data of *C. maxima* fruits during fruit development.

Supplementary Figure S2. The expression patterns of the 6 DELs identified in 5 comparisons.

Supplementary Figure S3. The top 20 GO terms of the potential target genes of DELs.

Supplementary Figure S4. Full length sequence of MSTRG.44863.1.

Supplementary Figure S5. Coding potential prediction of MSTRG.44863 calculated by Coding Potential Calculator.

Supplementary Figure S6. KEGG pathway enrichment analysis of DEGs after transient overexpression of MSTRG.44863.1.

Supplementary Figure S7. The total ion chromatograms of samples used for hormone assay.

Supplementary Figure S8. Transient silenced expression of MSTRG.44863.1 in pumpkin fruits.

Supplementary Figure S9. Transcription of MSTRG.44863.1 in vitro.

Supplementary Figure S10. Capillary shape of SAMS and MST traces.

Supplementary Figure S11. The content of SAM and activity of SAMS in EV-RNAi and MSTRG.44863.1-RNAi fruits.

Supplementary Figure S12. The expression of MSTRG.44863.1 was downregulated 4 h after IAA (100 mg/L) application.

Supplementary Figure S13. Pipeline for predicting lncRNAs.

Supplementary Table S1. Summary of *C. maxima* RNA-seq data.

Supplementary Table S2. Characteristics of all lncRNA identified by RNA-seq in this study.

Supplementary Table S3. List of known lncRNAs.

Supplementary Table S4. Differentially expressed lncRNAs.

Supplementary Table S5. The potential target genes of DELs.

Supplementary Table S6. Enriched GO terms of potential target genes.

Supplementary Table S7. lncRNAs corresponding to miRNA precursors.

Supplementary Table S8. The lncRNAs predicted as targets of miRNAs.

Supplementary Table S9. Targets of miRNAs verified by degradome sequencing.

Supplementary Table S10. DEGs after transient overexpression of MSTRG.44863.1.

Supplementary Table S11. KEGG pathway enrichment analysis of DEGs after transient overexpression of MSTRG.44863.1.

Supplementary Table S12. SNP and phenotypic data.

Supplementary Table S13. Potential target proteins of MSTRG.44863.1 identified by RNA pull-down assay.

Supplementary Table S14. The software and analysis website used in this study.

Supplementary Table S15. Primer sequences used in this study.

Funding

This work was supported by the Project of the National Natural Science Foundation of China (No. 31701940); the Youth Fund of Beijing Academy of Agriculture and Forestry Sciences (No. QNJJ202306); the Construction of cucurbits Collaboration and Innovation Center (XTCX202301); and Innovation and Development Program of the Beijing Vegetable Research Center (KYCX202303).

Conflict of interest statement. None declared.

Data availability

The data underlying this article are available in the article and in its online supplementary material.

Downloaded from https://academic.oup.com/plphys/article/195/2/940/7615931 by Beijing Academy of Agriculture & Forestry Sciences user on 31 October 2024

References

Abbas HMK, Huang H-X, Wang A-J, Wu T-Q, Xue S-D, Ahmad A, Xie D-S, Li J-X, Zhong Y-J. Metabolic and transcriptomic analysis of two *Cucurbita moschata* germplasms throughout fruit development. BMC Genomics. 2020:**21**(1):365. https://doi.org/10.1186/s12864-020-6774-y

Ai G, Li T, Zhu H, Dong X, Fu X, Xia C, Pan W, Jing M, Shen D, Xia A, et al. BPL3 binds the long non-coding RNA nalncFL7 to suppress FORKED-LIKE7 and modulate HAI1-mediated MPK3/6 dephosphorylation in plant immunity. Plant Cell. 2023:**35**(1):598–616. https://doi.org/10.1093/plcell/koac311

Bach-Pages M, Homma F, Kourelis J, Kaschani F, Mohammed S, Kaiser M, van der Hoorn RAL, Castello A, Preston GM. Discovering the RNA-binding proteome of plant leaves with an improved RNA interactome capture method. Biomolecules. 2020:**10**(4):661. https://doi.org/10.3390/biom10040661

Boualem A, Berthet S, Devani RS, Camps C, Fleurier S, Morin H, Troadec C, Giovinazzo N, Sari N, Dogimont C, et al. Ethylene plays a dual role in sex determination and fruit shape in cucurbits. Curr Biol. 2022:**32**(11):2390–2401. https://doi.org/10.1016/j.cub.2022.04.031

Bouvier F, Linka N, Isner JC, Mutterer J, Weber AP, Camara B. *Arabidopsis* SAMT1 defines a plastid transporter regulating plastid biogenesis and plant development. Plant Cell. 2006:**18**(11):3088–3105. https://doi.org/10.1105/tpc.105.040741

Carbonell-Bejerano P, Urbez C, Granell A, Carbonell J, Perez-Amador MA. Ethylene is involved in pistil fate by modulating the onset of ovule senescence and the GA-mediated fruit set in *Arabidopsis*. BMC Plant Biol. 2011:**11**:84. https://doi.org/10.1186/1471-2229-11-84

Chen C, Yang Y, Pan L, Xia W, Xu L, Hua B, Zhang Z, Miao M. Genome-wide identification of WD40 proteins in *Cucurbita maxima* reveals its potential functions in fruit development. Genes (Basel). 2023a:**14**(1):220. https://doi.org/10.3390/genes14010220

Chen D, Shao Q, Yin L, Younis A, Zheng B. Polyamine function in plants: metabolism, regulation on development, and roles in abiotic stress responses. Front Plant Sci. 2019:**9**:1945. https://doi.org/10.3389/fpls.2018.01945

Chen Y, Lu J, Wang W, Ch F, Yuan G, Sun J, Liu J, Wang C. Rose long noncoding RNA *lncWD83* promotes flowering by modulating ubiquitination of the floral repressor RcMYC2L. Plant Physiol. 2023b:**193**(4):2573–2591. https://doi.org/10.1093/plphys/kiad502

Dai X, Zhao PX. psRNATarget: a plant small RNA target analysis server. Nucleic Acids Res. 2011:**39**(suppl_2):W155–W159. https://doi.org/10.1093/nar/gkr319

Deng P, Liu S, Nie X, Song W, Wu L. Conservation analysis of long noncoding RNAs in plants. Sci China Life Sci. 2018:**61**(2):190–198. https://doi.org/10.1007/s11427-017-9174-9

Eddy SR. Non–coding RNA genes and the modern RNA world. Nat Rev Genet. 2001:**2**(12):919–929. https://doi.org/10.1038/35103511

Fenn MA, Giovannoni JJ. Phytohormones in fruit development and maturation. Plant J. 2021:**105**(2):446–458. https://doi.org/10.1111/tpj.15112

Gallart AP, Pulido AH, de Lagrán IAM, Sanseverino W, Cigliano RA. GREENC: a Wiki-based database of plant lncRNAs. Nucleic Acids Res. 2016:**44**(D1):D1161–D1166. https://doi.org/10.1093/nar/gkv1215

Gao C, Sun J, Dong Y, Wang C, Xiao S, Mo L, Jiao Z. Comparative transcriptome analysis uncovers regulatory roles of long non-coding RNAs involved in resistance to powdery mildew in melon. BMC Genomics. 2020:**21**:125. https://doi.org/10.1186/s12864-020-6546-8

Giovannoni JJ. Genetic regulation of fruit development and ripening. Plant Cell. 2004:**16**(suppl_1):S170–S180. https://doi.org/10.1105/tpc.019158

Hao Z, Fan C, Cheng T, Su Y, Wei Q, Li G. Genome-wide identification, characterization and evolutionary analysis of long intergenic noncoding RNAs in cucumber. PLoS One. 2015:**10**(3):e0121800. https://doi.org/10.1371/journal.pone.0121800

Hosen M, Rafii MY, Mazlan N, Jusoh M, Oladosu Y, Chowdhury MFN, Muhammad I, Khan MMH. Pumpkin (Cucurbita spp.): a crop to mitigate food and nutritional challenges. Horticulturae. 2021:**7**(10):352. https://doi.org/10.3390/horticulturae7100352

Huang W, Hu N, Xiao Z, Qiu Y, Yang Y, Yang J, Mao X, Wang Y, Li Z, Guo H. A molecular framework of ethylene-mediated fruit growth and ripening processes in tomato. Plant Cell. 2022:**34**(9):3280–3300. https://doi.org/10.1093/plcell/koac146

Jerabek-Willemsen M, Wienken CJ, Braun D, Baaske P, Duhr S. Molecular interaction studies using microscale thermophoresis. Assay Drug Dev Technol. 2011:**9**(4):342–353. https://doi.org/10.1089/adt.2011.0380

Jia H, Osak M, Bogu GK, Stanton LW, Johnson R, Lipovich L. Genome-wide computational identification and manual annotation of human long noncoding RNA genes. RNA. 2010:**16**(8):1478–1487. https://doi.org/10.1261/rna.1951310

Jiang N, Cui J, Shi Y, Yang G, Zhou X, Hou X, Meng J, Luan Y. Tomato lncRNA23468 functions as a competing endogenous RNA to modulate *NBS-LRR* genes by decoying miR482b in the tomato-*Phytophthora infestans* interaction. Hortic Res. 2019:**6**:28. https://doi.org/10.1038/s41438-018-0096-0

Kang C, Liu Z. Global identification and analysis of long noncoding RNAs in diploid strawberry *Fragaria vesca* during flower and fruit development. BMC Genomics. 2015:**16**:815. https://doi.org/10.1186/s12864-015-2014-2

Kapranov P, Cheng J, Dike S, Nix DA, Duttagupta R, Willingham AT, Stadler PF, Hertel J, Hackermüller J, Hofacker IL, et al. RNA maps reveal new RNA classes and a possible function for pervasive transcription. Science. 2007:**316**(5830):1484–1488. https://doi.org/10.1126/science.1138341

Kim D, Langmead B, Salzberg SL. HISAT: a fast spliced aligner with low memory requirements. Nat Methods. 2015:**12**(4):357–360. https://doi.org/10.1038/nmeth.3317

Kumar R, Khurana A, Sharma AK. Role of plant hormones and their interplay in development and ripening of fleshy fruits. J Exp Bot. 2014:**65**(16):4561–4575. https://doi.org/10.1093/jxb/eru277

Li H, Durbin R. Fast and accurate short read alignment with Burrows-Wheeler transform. Bioinformatics. 2009:**25**(14):1754–1760. https://doi.org/10.1093/bioinformatics/btp324

Li H, Handsaker B, Wysoker A, Fennell T, Ruan J, Homer N, Marth G, Abecasis G, Durbin R. The sequence alignment/map format and SAMtools. Bioinformatics. 2009:**25**(16):2078–2079. https://doi.org/10.1093/bioinformatics/btp352

Li J, Ma W, Zeng P, Wang J, Geng B, Yang J, Cui Q. LncTar: a tool for predicting the RNA targets of long noncoding RNAs. Brief Bioinform. 2015:**16**(5):806–812. https://doi.org/10.1093/bib/bbu048

Li L, Eichten SR, Shimizu R, Petsch K, Yeh C-T, Wu W, Chettoor AM, Givan SA, Cole RA, Fowler JE, et al. Genome-wide discovery and characterization of maize long non-coding RNAs. Genome Biol. 2014:**15**(2):R40. https://doi.org/10.1186/gb-2014-15-2-r40

Li N, Wang Y, Zheng R, Song X. Research progress on biological functions of lncRNAs in major vegetable crops. Veg Res. 2022a:**2**(1):1–14. https://doi.org/10.48130/VR-2022-0014

Li R, Fu D, Zhu B, Luo Y, Zhu H. CRISPR/Cas9-mediated mutagenesis of lncRNA1459 alters tomato fruit ripening. Plant J. 2018:**94**(3):513–524. https://doi.org/10.1111/tpj.13872

Li W, Chen Y, Wang Y, Zhao J, Wang Y. Gypsy retrotransposon-derived maize lncRNA GARR2 modulates gibberellin response. Plant J. 2022b:**110**(5):1433–1446. https://doi.org/10.1111/tpj.15748

Lindermayr C, Rudolf EE, Durner J, Groth M. Interactions between metabolism and chromatin in plant models. Mol Metab. 2020:**38**:100951. https://doi.org/10.1016/j.molmet.2020.01.015

Liu F, Marquardt S, Lister C, Swiezewski S, Dean C. Targeted 3′ processing of antisense transcripts triggers *Arabidopsis FLC* chromatin silencing. Science. 2010:**327**(5961):94–97. https://doi.org/10.1126/science.1180278

Downloaded from https://academic.oup.com/plphys/article/195/2/940/7615931 by Beijing Academy of Agriculture & Forestry Sciences user on 31 October 2024

Liu J, Jung C, Xu J, Wang H, Deng S, Bernad L, Arenas-Huertero C, Chua N-H. Genome-wide analysis uncovers regulation of long intergenic noncoding RNAs in *Arabidopsis*. Plant Cell. 2012:**24**(11): 4333–4345. https://doi.org/10.1105/tpc.112.102855

Liu M, Diretto G, Pirrello J, Roustan J-P, Li Z, Giuliano G, Regadn F, Bouzayen M. The chimeric repressor version of an Ethylene Response Factor (ERF) family member, Sl-ERF.B3, shows contrasting effects on tomato fruit ripening. New Phytol. 2014:**203**(1):206–218. https://doi.org/10.1111/nph.12771

Livak KJ, Schmittgen TD. Analysis of relative gene expression data using real-time quantitative PCR and the $2^{-\Delta\Delta Ct}$ method. Methods. 2001:**25**(4):402–408. https://doi.org/10.1006/meth.2001.1262

Lucero L, Ferrero L, Fonouni-Farde C, Ariel F. Functional classification of plant long noncoding RNAs: a transcript is known by the company it keeps. New Phytol. 2021:**229**(3):1251–1260. https://doi.org/10.1111/nph.16903

Luo Y, Wang C, Wang M, Wang Y, Xu W, Han H, Wang Z, Zhong Y, Huang H, Qu S. Accumulation of carotenoids and expression of carotenoid biosynthesis genes in fruit flesh during fruit development in two *Cucurbita maxima* inbred lines. Hortic Plant J. 2021:**7**(6): 529–538. https://doi.org/10.1016/j.hpj.2020.07.006

Ma H, Yang T, Li Y, Zhang J, Wu T, Song T, Yao Y, Tian J. The long noncoding RNA MdLNC499 bridges MdWRKY1 and MdERF109 function to regulate early-stage light-induced anthocyanin accumulation in apple fruit. Plant Cell. 2021:**33**(10):3309–3330. https://doi.org/10.1093/plcell/koab188

Martel C, Vrebalov J, Tafelmeyer P, Giovannoni JJ. The tomato MADS-box transcription factor RIPENING INHIBITOR interacts with promoters involved in numerous ripening processes in a COLORLESS NONRIPENING-dependent manner. Plant Physiol. 2011:**157**(3):1568–1579. https://doi.org/10.1104/pp.111.181107

Martínez C, Manzano S, Megías Z, Garrido D, Picó B, Jamilena M. Involvement of ethylene biosynthesis and signalling in fruit set and early fruit development in zucchini squash (*Cucurbita pepo* L.). BMC Plant Biol. 2013:**13**:139. https://doi.org/10.1186/1471-2229-13-139

Ozga JA, Reinecke DM. Hormonal interactions in fruit development. J Plant Growth Regul. 2003:**22**(1):73–81. https://doi.org/10.1007/s00344-003-0024-9

Papoutsisa K, Zhang J, Bowyer MC, Brunton N, Gibney ER, Lynga J. Fruit, vegetables, and mushrooms for the preparation of extracts with α-amylase and α-glucosidase inhibition properties: a review. Food Chem. 2021:**338**:128119. https://doi.org/10.1016/j.foodchem.2020.128119

Pauli A, Valen E, Lin MF, Garber M, Vastenhouw NL, Levin JZ, Fan L, Sandelin A, Rinn JL, Regev A. Systematic identification of long noncoding RNAs expressed during Zebrafish embryogenesis. Genome Res. 2012:**22**(3):577–591. https://doi.org/10.1101/gr.133009.111

Pertea M, Kim D, Pertea GM, Leek JT, Salzberg SL. Transcript-level expression analysis of RNA-seq experiments with HISAT, StringTie and Ballgown. Nat Protoc. 2016:**11**(9):1650–1667. https://doi.org/10.1038/nprot.2016.095

Qin T, Zhao H, Cui P, Albesher N, Xiong L. A nucleus-localized long noncoding RNA enhances drought and salt stress tolerance. Plant Physiol. 2017:**175**(3):1321–1336. https://doi.org/10.1104/pp.17.00574

Quinet M, Angosto T, Yuste-Lisbona FJ, Blanchard-Gros R, Bigot S, Martinez J-P, Lutts S. Tomato fruit development and metabolism. Front Plant Sci. 2019:**10**:1554. https://doi.org/10.3389/fpls.2019.01554

Roberts A, Pimentel H, Trapnell C, Pachter L. Identification of novel transcripts in annotated genomes using RNA-Seq. Bioinformatics. 2011:**27**(17):2325–2329. https://doi.org/10.1093/bioinformatics/btr355

Rocha PSCF, Sheikh M, Melchiorre R, Fagard M, Boutet S, Loach R, Moffatt B, Wagner C, Vaucheret H, Furner I. The *Arabidopsis* HOMOLOGYDEPENDENT GENE SILENCING1 gene codes for an S-adenosyl-Lhomocysteine hydrolase required for DNA methylation-dependent gene silencing. Plant Cell. 2005:**17**(2):404–417. https://doi.org/10.1105/tpc.104.028332

Sharma K, Gupta S, Sarma S, Rai M, Sreelakshmi Y, Sharma R. Mutations in tomato 1-aminocyclopropane carboxylic acid synthase2 uncover its role in development beside fruit ripening. Plant J. 2021:**106**(1):95–112. https://doi.org/10.1111/tpj.15148

Shinozaki Y, Hao S, Kojima M, Sakakibara H, Ozeki-Iida Y, Zheng Y, Fei Z, Zhong S, Giovannoni JJ, Rose JKC, et al. Ethylene suppresses tomato (*Solanum lycopersicum*) fruit set through modification of gibberellin metabolism. Plant J. 2015:**83**(2):237–251. https://doi.org/10.1111/tpj.12882

Song X, Hu J, Wu T, Yang Q, Feng X, Lin H, Feng S, Cui C, Yu Y, Zhou R, et al. Comparative analysis of long noncoding RNAs in angiosperms and characterization of long noncoding RNAs in response to heat stress in Chinese cabbage. Hortic Res. 2021:**8**(1):48. https://doi.org/10.1038/s41438-021-00484-4

Stevenson DG, Yoo SH, Hurst PL, Jane JL. Structural and physicochemical characteristics of winter squash (*Cucurbita maxima* D.) fruit starches at harvest. Carbohydr Polym. 2005:**59**(2):153–163. https://doi.org/10.1016/j.carbpol.2004.08.030

Storey JD. A direct approach to false discovery rates. J R Stat Soc B. 2002:**64**(3):479–498. https://doi.org/10.1111/1467-9868.00346

Sun H, Wu S, Zhang G, Jiao C, Guo S, Ren Y, Zhang J, Zhang H, Gong G, Jia Z, et al. Karyotype stability and unbiased fractionation in the paleo-allotetraploid *Cucurbita* genomes. Mol Plant. 2017:**10**(10): 1293–1306. https://doi.org/10.1016/j.molp.2017.09.003

Sun L, Luo H, Bu D, Zhao G, Yu K, Zhang C, Liu Y, Chen R, Zhao Y. Utilizing sequence intrinsic composition to classify protein-coding and long non-coding transcripts. Nucleic Acids Res. 2013:**41**(17): e166. https://doi.org/10.1093/nar/gkt646

Szcześniak MW, Rosikiewicz W, Makałowska I. CANTATAdb: a collection of plant long non-coding RNAs. Plant Cell Physiol. 2016:**57**(1):e8. https://doi.org/10.1093/pcp/pcv201

Tang Y, Qu Z, Lei J, He R, Adelson DL, Zhu Y, Yang Z, Wang D. The long noncoding RNA *FRILAIR* regulates strawberry fruit ripening by functioning as a noncanonical target mimic. PLoS Genet. 2021:**17**(3): e1009461. https://doi.org/10.1371/journal.pgen.1009461

Tian J, Zhang G, Zhang F, Ma J, Wen C, Li H. Genome-wide identification of powdery mildew responsive long non-coding RNAs in *Cucurbita pepo*. Front Genet. 2022:**13**:933022. https://doi.org/10.3389/fgene.2022.933022

Tian Y, Bai S, Dang Z, Hao J, Zhang J, Hasi A. Genome-wide identification and characterization of long non-coding RNAs involved in fruit ripening and the climacteric in *Cucumis melo*. BMC Plant Biol. 2019:**19**(1):369. https://doi.org/10.1186/s12870-019-1942-4

Vriezen WH, Feron R, Maretto F, Keijman J, Mariani C. Changes in tomato ovary transcriptome demonstrate complex hormonal regulation of fruit set. New Phytol. 2008:**177**(1):60–76. https://doi.org/10.1111/j.1469-8137.2007.02254.x

Wang C, Li Y, Yan S, Wang H, Shao X, Xiao M, Yang B, Qin G, Kong R, Chen R, et al. Interactome analysis reveals that lncRNA HULC promotes aerobic glycolysis through LDHA and PKM2. Nat Commun. 2020a:**11**(1):3162. https://doi.org/10.1038/s41467-020-16966-3

Wang C, Wang Y, Wang M, Han H, Luo Y, Ding W, Xu W, Zhong Y, Huang H, Qu S. Soluble sugars accumulation and related gene expression during fruit development in *Cucurbita maxima* Duchesne. Sci Hortic. 2020b:**272**:109520. https://doi.org/10.1016/j.scienta.2020.109520

Wang H, Chung PJ, Liu J, Jang I-C, Kean MJ, Xu J, Chua N-H. Genome-wide identification of long noncoding natural antisense transcripts and their responses to light in *Arabidopsis*. Genome Res. 2014:**24**(3):444–453. https://doi.org/10.1101/gr.165555.113

Wang H, Schauer N, Usadel B, Frasse P, Zouine M, Hernould M, Latché A, Pech J-C, Fernie AR, Bouzayen M. Regulatory features underlying pollination-dependent and -independent tomato fruit set revealed by transcript and primary metabolite profiling. Plant Cell. 2009:**21**(5):1428–1452. https://doi.org/10.1105/tpc.108.060830

Wang M, Zhao W, Gao L, Zhao L. Genome-wide profiling of long non-coding RNAs from tomato and a comparison with mRNAs

Downloaded from https://academic.oup.com/plphys/article/195/2/940/7615931 by Beijing Academy of Agriculture & Forestry Sciences user on 31 October 2024

associated with the regulation of fruit ripening. BMC Plant Biol. 2018:**18**(1):75. https://doi.org/10.1186/s12870-018-1300-y

Waseem M, Liu Y, Xia R. Long non-coding RNAs, the dark matter: an emerging regulatory component in plants. Int J Mol Sci. 2020:**22**(1): 86. https://doi.org/10.3390/ijms22010086

Wu H-J, Wang Z-M, Wang M, Wang X-J. Widespread long noncoding RNAs as endogenous target mimics for microRNAs in plants. Plant Physiol. 2013:**161**(4):1875–1884. https://doi.org/10.1104/pp.113.215962

Wu L, Liu S, Qi H, Cai H, Xu M. Research progress on plant long noncoding RNA. Plants. 2020:**9**(4):408. https://doi.org/10.3390/plants9040408

Wyatt LE, Strickler SR, Mueller LA, Mazourek M. Comparative analysis of *Cucurbita pepo* metabolism throughout fruit development in acorn squash and oilseed pumpkin. Hortic Res. 2016:**3**(1):16045. https://doi.org/10.1038/hortres.2016.45

Xie C, Mao X, Huang J, Ding Y, Wu J, Dong S, Kong L, Gao G, Li C-Y, Wei L. KOBAS 2.0: a web server for annotation and identification of enriched pathways and diseases. Nucleic Acids Res. 2011: **39**(suppl_2):W316–W322. https://doi.org/10.1093/nar/gkr483

Xin T, Zhang Z, Li S, Zhang S, Li Q, Zhang Z-H, Huang S, Yang X. Genetic regulation of ethylene dosage for Cucumber fruit elongation. Plant Cell. 2019:**31**(5):1063–1076. https://doi.org/10.1105/tpc.18.00957

Yan Z, Shi J, Gao L, Wang Q, Zuo J. The combined treatment of broccoli florets with kojic acid and calcium chloride maintains postharvest quality and inhibits off-odor production. Sci Hortic. 2020:**262**:109019. https://doi.org/10.1016/j.scienta.2019.109019

Yang T, Ma H, Zhang J, Wu T, Song T, Tian J, Yao Y. Systematic identification of long noncoding RNAs expressed during light-induced anthocyanin accumulation in apple fruit. Plant J. 2019:**100**(3): 572–590. https://doi.org/10.1111/tpj.14470

Yu J, Qiu K, Sun W, Yang T, Wu T, Song T, Zhang J, Yao Y, Tian J. A long noncoding RNA functions in high-light-induced anthocyanin accumulation in apple by activating ethylene synthesis. Plant Physiol. 2022:**189**(1):66–83. https://doi.org/10.1093/plphys/kiac049

Zhang B, Su T, Li P, Xin X, Cao Y, Wang W, Zhao X, Zhang D, Yu Y, Li D, et al. Identification of long noncoding RNAs involved in resistance to downy mildew in Chinese cabbage. Hortic Res. 2021:**8**(1):44. https://doi.org/10.1038/s41438-021-00479-1

Zhang G, Chen D, Zhang T, Duan A, Zhang J, He C. Transcriptomic and functional analyses unveil the role of long non-coding RNAs in anthocyanin biosynthesis during sea buckthorn fruit ripening. DNA Res. 2018:**25**(5):465–476. https://doi.org/10.1093/dnares/dsy017

Zhang L, Liu J, Cheng J, Sun Q, Zhang Y, Liu J, Li H, Zhang Z, Wang P, Cai C, et al. lncRNA7 and lncRNA2 modulate cell wall defense genes to regulate cotton resistance to Verticillium wilt. Plant Physiol. 2022:**189**(1):264–284. https://doi.org/10.1093/plphys/kiac041

Zhang Y-C, Liao J-Y, Li Z-Y, Yu Y, Zhang J-P, Li Q-F, Qu L-H, Shu W-S, Chen Y-Q. Genome-wide screening and functional analysis identify a large number of long noncoding RNAs involved in the sexual reproduction of rice. Genome Biol. 2014:**15**(12):512. https://doi.org/10.1186/s13059-014-0512-1

Zhang Z, Chen H, Huang X, Xia R, Zhao Q, Lai J, Teng K, Li Y, Liang L, Du Q, et al. BSCTV c2 attenuates the degradation of SAMDC1 to suppress DNA methylation-mediated gene silencing in *Arabidopsis*. Plant Cell. 2011:**23**(1):273–288. https://doi.org/10.1105/tpc.110.081695

Zhong Y-J, Huang J-C, Liu J, Li Y, Jiang Y, Xu Z-F, Sandmann G, Chen F. Functional characterization of various algal carotenoid ketolases reveals that ketolating zeaxanthin efficiently is essential for high production of astaxanthin in transgenic *Arabidopsis*. J Exp Bot. 2011:**62**(10):3659–3669. https://doi.org/10.1093/jxb/err070

Zhong Y-J, Zhou Y-Y, Li J-X, Yu T, Wu T-Q, Luo J-N, Luo S-B, Huang H-X. A high-density linkage map and QTL mapping of fruit-related traits in pumpkin (*Cucurbita moschata* Duch.). Sci Rep. 2017:**7**(1): 12785. https://doi.org/10.1038/s41598-017-13216-3

Zhu B, Yang Y, Li R, Fu D, Wen L, Luo Y, Zhu H. RNA sequencing and functional analysis implicate the regulatory role of long non-coding RNAs in tomato fruit ripening. J Exp Bot. 2015:**66**(15):4483–4495. https://doi.org/10.1093/jxb/erv203

Zhu Q-H, Stephen S, Taylor J, Helliwell CA, Wang M-B. Long noncoding RNAs responsive to *Fusarium oxysporum* infection in *Arabidopsis thaliana*. New Phytol. 2014:**201**(2):574–584. https://doi.org/10.1111/nph.12537

Downloaded from https://academic.oup.com/plphys/article/195/2/940/7615931 by Beijing Academy of Agriculture & Forestry Sciences user on 31 October 2024